NEOPLASIA
www.neoplasia.com

Volume 14 Number 8 August 2012 pp. 757–770 757

Plasmacytoid Dendritic Cells in the Tumor Microenvironment: Immune Targets for Glioma Therapeutics[1,2]

Marianela Candolfi[*,3], Gwendalyn D. King[*], Kader Yagiz[*], James F. Curtin[*], Yohei Mineharu[*], AKM Ghulam Muhammad[*], David Foulad[*], Kurt M. Kroeger[*,4], Nick Barnett[*], Regis Josien[†], Pedro R. Lowenstein[*,‡] and Maria G. Castro[*,‡]

*Gene Therapeutics Research Institute, Cedars Sinai Medical Center, and Departments of Molecular and Medical Pharmacology, and Medicine, David Geffen School of Medicine, University of California Los Angeles, Los Angeles, CA; [†]Institut National de la Sante et de la Recherche Medicale (INSERM) U437 and ITERT, Nantes, France; [‡]Department of Neurosurgery, Department of Cell and Developmental Biology, University of Michigan School of Medicine, Ann Arbor, MI

Abstract

Adenovirus-mediated delivery of the immune-stimulatory cytokine Flt3L and the conditionally cytotoxic thymidine kinase (TK) induces tumor regression and long-term survival in preclinical glioma (glioblastoma multiforme [GBM]) models. Flt3L induces expansion and recruitment of plasmacytoid dendritic cells (pDCs) into the brain. Although pDCs can present antigen and produce powerful inflammatory cytokines, that is, interferon α (IFN-α), their role in tumor immunology remains debated. Thus, we studied the role of pDCs and IFN-α in Ad.TK/GCV + Ad.Flt3L–mediated anti-GBM therapeutic efficacy. Our data indicate that the combined gene therapy induced recruitment of plasmacytoid DCs (pDCs) into the tumor mass; which were capable of *in vivo* phagocytosis, IFN-α release, and T-cell priming. Thus, we next used either pDCs or an Ad vector encoding IFN-α delivered within the tumor microenvironment. When rats were treated with Ad.TK/GCV in combination with pDCs or Ad-IFN-α, they exhibited 35% and 50% survival, respectively. However, whereas intracranial administration of Ad.TK/GCV + Ad.Flt3L exhibited a high safety profile, Ad-IFN-α led to severe local inflammation, with neurologic and systemic adverse effects. To elucidate whether the efficacy of the immunotherapy was dependent on IFN-α–secreting pDCs, we administered an Ad vector encoding B18R, an IFN-α antagonist, which abrogated the antitumoral effect of Ad.TK/GCV + Ad.Flt3L. Our data suggest that IFN-α release by activated pDCs plays a critical role in the antitumor effect mediated by Ad.TK/GCV + Ad.Flt3L. In summary, taken together, our results demonstrate that pDCs mediate anti-GBM therapeutic efficacy through the production of IFN-α, thus manipulation of pDCs constitutes an attractive new therapeutic target for the treatment of GBM.

Neoplasia (2012) 14, 757–770

Abbreviations: Ad, adenoviral vector; APC, antigen-presenting cell; DC, dendritic cell; dLN, draining lymph node; Flt3L, *fms*-like tyrosine kinase 3; GBM, glioblastoma multiforme; IFN-α, interferon α; MHC, major histocompatibility complex; pDC, plasmacytoid dendritic cell; TK, thymidine kinase; TLR, Toll-like receptor

Address all correspondence to: Maria G. Castro, PhD, Department of Neurosurgery, Department of Cell and Developmental Biology, University of Michigan School of Medicine, 4570 MSRB II, 1150 W Medical Center Dr, Ann Arbor, MI 48109-5689. E-mail: mariacas@umich.edu

[1]Our work was supported by National Institutes of Health/National Institute of Neurological Disorders & Stroke (NIH/NINDS) grants 1UO1 NS052465, UO1-NS052465-04S1, 1RO1-NS057711, and 1RO1-NS074387 to M.G.C.; NIH/NINDS grants 1RO1-NS 054193; and 1RO1-NS061107 to P.R.L.; The Bram and Elaine Goldsmith and the Medallions Group Endowed Chairs in Gene Therapeutics to P.R.L. and M.G.C., respectively, the Board of Governors at CSMC and the Department of Neurosurgery, University of Michigan School of Medicine. M.C. was supported by an NIH/NINDS 1F32 NS058156 fellowship and the National Council of Science and Technology (CONICET, Argentina).

[2]This article refers to supplementary materials, which are designated by Figures W1 to W5 and are available online at www.neoplasia.com.

[3]Current address: Instituto de Investigaciones Biomédicas, INBIOMED, Facultad de Medicina, Universidad de Buenos Aires, Paraguay 2155, piso 10, CP 1421 Buenos Aires, Argentina.

[4]Deceased.

Received 8 May 2012; Revised 10 July 2012; Accepted 11 July 2012

DOI 10.1593/neo.12794

Introduction

Glioblastoma multiforme (GBM) is the most common and aggressive primary brain tumor. Its invasiveness in the surrounding nonneoplastic brain and its intrinsic resistance to traditional therapeutic approaches make this disease a therapeutic challenge [1–4]. Several therapeutic approaches have attempted to stimulate the immune system to target and kill GBM cells. To this end, interferon α (IFN-α) has recently been proposed for the treatment of GBM owing to its effects on antitumor immunity, angiogenesis, and tumor cell proliferation and death [5–8]. IFN-α has shown a direct antitumor effect by reducing angiogenesis in GBM growing in the rat brain [7], inhibiting the proliferation of GBM cells [9] and sensitizing them to proapoptotic agents [10]. IFN-α has also shown indirect antitumor activity in several types of cancers through the stimulation of the host immune system: it can activate dendritic cells (DCs), upregulate major histocompatibility complex (MHC) types I and II expression, increase the recruitment of immune cells into the tumor microenvironment, and enhance cellular and humoral antitumor immunity [6]. Although IFN-α was the first cytokine to be approved for cancer treatment, its considerable toxicity has limited its use [11,12].

Our efforts toward developing an immunotherapeutic approach for the treatment of GBM that would be highly effective and nontoxic to the surrounding brain parenchyma consist of the delivery of a conditional cytotoxic molecule and a cytokine using adenoviral vectors (Ads) [13–16]. One Ad encodes Herpes simplex virus 1 thymidine kinase (Ad.TK), which kills proliferating cells in the presence of ganciclovir, and the second Ad encodes *fms*-like tyrosine kinase 3 ligand (Ad.Flt3L), which recruits antigen-presenting cells (APCs) to the brain tumor microenvironment [17]. This combined gene therapy eradicates established intracranial tumors in several rat and mouse preclinical GBM models [18]. We have previously shown that this treatment induces an antitumor immune response that is dependent on APCs, $CD4^+$, and $CD8^+$ T cells [14,19,20].

Flt3L is a growth factor that induces the expansion of DCs [21]. Our previous results have shown that intracranial administration of an Ad encoding Flt3L (Ad.Flt3L) induces the expansion and recruitment of plasmacytoid DCs (pDCs), which are a subset of IFN-α–producing DCs, into the rat brain parenchyma [22]. The role of pDCs in tumor immunology remains debated because it has been reported that pDCs can induce immunologic tolerance or antitumor immunity [23]. In patients with head and neck squamous cell carcinoma, tumor-infiltrating pDCs were found to have a decreased response to Toll-like receptor 9 (TLR9) activation [24]. pDCs detected in ovarian cancer were involved in the generation of an immunosuppressive tumor microenvironment [25] and the promotion of tumor angiogenesis [26].

pDCs can mature and express costimulatory molecules and inflammatory cytokines and migrate to the draining lymph nodes (dLNs) to present tumor antigens to naive $CD4^+$ T cells [23]. Although there is evidence that pDCs have the ability to present antigens, their main role seems to be as IFN-α–producing cells [27]. pDCs are considered the professional IFN-α–producing cells, being able to release between 100 to 1000 times more type I IFN than other immune cells after activation [27]. Here we aimed to elucidate the role of pDCs in the antitumor immune response mediated by Ad.TK + Ad.Flt3L. Thus, we assessed the ability of intratumoral pDCs to uptake and transport tumor cell remnants. We also purified tumor-infiltrating pDCs and characterized the expression of costimulatory molecules and their ability to prime T cells and produce inflammatory cytokines.

Because here we demonstrate that treatment with Ad.TK + Ad.Flt3L induces the recruitment of IFN-α–producing pDCs into the brain tumor mass, we hypothesized that this cytokine could play a critical role in mediating the antitumor therapeutic efficacy elicited by this treatment. Our data suggest that IFN-α release by activated pDCs mediates antitumor effects elicited by Ad.TK/GCV + Ad.Flt3L gene therapy. Therefore, manipulation of pDCs constitutes an attractive novel target for the treatment of GBM.

Materials and Methods

Adenoviral Vectors

The vectors used in this study were first-generation, replication-deficient, recombinant adenovirus type 5 vectors (Ad), with deletion in the E1 and E3 regions; the expression cassette containing the appropriate transgene is inserted within the E1 region [28]. Five Ad vectors were used: Ad.TK (encodes HSV1-thymidine kinase under the control of the human CMV promoter [14,19]), Ad.Flt3L (encodes human soluble *fms*-like tyrosine kinase ligand under the control of the human CMV promoter [14,17,19,22,29]), Ad.IFN-α (kindly donated by Dr Kazunori Aoki, National Cancer Center Research Institute, Tokyo, Japan; it encodes rat IFN-α under the control of the CAG promoter, which combines the human cytomegalovirus immediate-early enhancer and a modified chicken β-actin promoter [30]), Ad.B18R (encodes B18R an IFN-α decoy receptor under the control of the murine CMV promoter [31]), and, as a control, we used an Ad without transgene (Ad.0 [14]). For the generation of Ad.B18R, the *B18R* gene was polymerase chain reaction amplified from purified Vaccinia viral DNA (kind gift from Dr R Mark L. Buller, Saint Luis University, MO [31]) using the following primers: B18R-for ccgctcgaggatatcgtcgacATGAGTCGTCGTCTGATT (5′ overhangs containing *Xho*I, *Eco*RV, and *Sal*I restriction sites) and B18R-rev ccgctcgaggactagtgtcgacCTATACTTTGGTAGGTGG (3′ overhangs containing *Xho*I, *Spe*I, and *Sal*I restriction sites). Thirty thermal cycles (94°C denature, 55°C anneal, 72°C extension) were performed using an Applied Biosystems thermocycler (Foster City, CA). The polymerase chain reaction product was purified (Qiagen, Hilden, Germany) and cloned into pGEM-T-easy vector (Promega, Madison, WI). The *B18R* gene was excised with *Xho*I and cloned into the *Sal*I site of pAL120, an adenoviral shuttle plasmid containing the powerful murine CMV promoter in the E1 region of adenovirus [32] to generate pAL120-B18R. 293 cells were co-transfected with pAL120-B18R and pJM17 (Microbix, Toronto, Canada) using TransIT-293 Transfection Reagent (Mirus Bio, Madison, WI) to rescue the viral vector. Ad-mCMV-B18R was amplified and purified as described by us previously [28]. All viral preparations were tested free of replication-competent adenovirus and lipopolysaccharide contamination using methods previously described [28].

Rat GBM Model

Rats were housed in a pathogen-free environment and humidity and temperature–controlled vivarium on a 12:12-hour light/dark cycle (lights on 7:00 A.M.) with free access to food and water. All animal experiments were performed after prior approval by the Institutional Animal Care and Use Committee at Cedars-Sinai Medical Center and conformed to the policies and procedures of the Comparative Medicine Department. After administration of anesthesia, animals were placed in a stereotactic apparatus and injected unilaterally into the right striatum. Rats were injected using a 10-μl Hamilton syringe (coordinates: 1 mm forward from bregma and 3.1 mm lateral). Animals were allowed to recover, and their health status was closely monitored. CNS-1 cells (4500) were injected as described before [33]. CNS-1 cells were grown in Dulbecco modified Eagle culture medium

(CellGro, Herndon, VA), supplemented with 10% fetal calf serum, 1% L-glutamine, 1% Pen-Strep, 1% nonessential amino acids, and passaged routinely. On the day of surgery, cells were trypsinized, resuspended in Dulbecco modified Eagle medium without supplements (1500 cells/μl) and kept on ice for up to 2 hours.

Ad vectors were administered 10 days after tumor implantation at a dose of 5×10^7 each in a volume of 3 μl, using the same drill hole and delivered in three locations ventral of the dura: 5.5, 5.0, and 4.5 mm into the tumor mass (1 μl per site). The total viral load in each injection was standardized by the addition of Ad.0 when single viruses were administered (total dose, 10^8 pfu). Twenty-four hours after delivery of viral vectors, animals that received Ad.TK began treatment with GCV (7 mg/100 μl intraperitoneally), twice daily for 7 days. Animals were monitored daily and killed according to the guidelines of the Institutional Animal Care and Use Committee at Cedars-Sinai Medical Center at the first signs of moribund behavior or at predetermined time points for collection of tumor-infiltrating immune cells, immunofluorescence, or neuropathology. Animals were killed under deep anesthesia by terminal perfusion with Tyrodes solution (132 mM NaCl, 1.8 mM $CaCl_2$, 0.32 mM NaH_2PO_4, 5.56 mM glucose, 11.6 mM $NaHCO_3$, and 2.68 mM KCl) followed by perfusion with 4% paraformaldehyde (PFA) when tissues were to be used for immunofluorescence or neuropathology. Brains were removed and further fixed in 4% PFA for 4 to 5 days or processed for flow cytometry.

A set of tumor-bearing rats was injected with 2×10^7 yellow-green FluoSpheres (1 μm; catalog no. F-13081; Molecular Probes, Eugene, OR) in a total volume of 4 μl (1 μl each delivered at four locations ventral to the dura: −5.25, −4.75, −4.25, and −3.75) 3 days after the treatment with Ad.TK + Ad.Flt3L. Rats were killed 2 and 5 days later and the brains and cervical lymph nodes were collected to detect phagocytic activity *in vivo*. Brains and cervical lymph nodes were collected and postfixed for 72 hours. A set of naive rats was injected with the Ad vectors in the brain as described above for neuropathologic analysis. They were weighted daily and killed 7 and 60 days after injection.

Identification of Tumor-Infiltrating Immune Cells

At 5 and 12 days after treatment, brains from tumor-bearing rats were carefully separated from the meninges with scissors and removed from the skull. Tumors were carefully dissected with a scalpel blade and removed avoiding the ventricles. The tumor tissue was diced with a razor blade before homogenizing in supplemented RPMI medium (containing 10% fetal bovine serum, 1% penicillin/streptomycin (PS), 1% L-glutamine) using a glass Tenbroeck homogenizer (Kontes, Vineland, NJ). Mononuclear cells were purified from brain tissue by centrifugation (2200 rpm) through a Percoll step gradient (70% to 30% Percoll in phosphate-buffered saline [PBS]) for 20 minutes in 15-ml falcon tubes (GE Healthcare, Piscataway, NJ); mononuclear cells migrate to the interface between 30% and 70% Percoll. The mononuclear cells on the interphase were removed into 10-ml fresh medium, washed, and counted using Trypan blue. Tumor-infiltrating immune cells were labeled with antibodies in cell surface staining buffer (0.1 M PBS, without Ca^{2+} and Mg^{2+}, with 1% fetal bovine serum) for analysis by flow cytometry using a FACScan flow cytometer (Becton Dickinson, San Jose, CA). To identify the immune cell populations, we used the following antibodies (BD Biosciences, San Diego, CA): pDCs and B cells were detected by labeling with mouse antirat CD3-FITC, mouse antirat CD4-PECy5, and mouse antirat CD45R-PE (catalog nos. 559975, 554839 and 554881, respectively; BD Pharmingen). NK, NK-T, and T cells were detected by labeling with mouse antirat CD3-FITC and mouse antirat CD161a-PE (catalog nos. 559975 and 555006, respectively; BD Pharmingen). Macrophages were detected by labeling with mouse antirat CD68.ED1-$Alexa_{488}$ (catalog no. MCA341A488; Serotec, Oxford, United Kingdom) after 4% paraformaldehyde fixation. Microglia was identified by labeling with mouse antirat CD45-PE (catalog no. 554878; BD Pharmingen). Conventional DCs (cDCs) were detected by labeling with mouse antirat CD11c-FITC (catalog no. MCA1441F; Serotec), MHC II–PerCP and CD45-PE (catalog nos. 557016 and 554878; BD Pharmingen). In all instances, tumor-infiltrating populations were determined based on gating established with naive splenic populations. Spleens were harvested and homogenized in glass Tenbroeck homogenizer. Red blood cells were removed by incubating in 3 ml of ACK solution (0.15 mM NH_4Cl, 10 mM $KHCO_3$, and 0.1 mM sodium EDTA at pH 7.2) for 3 minutes on ice. Splenocytes were then washed in supplemented RPMI medium and processed in parallel with tumor-infiltrating immune cells for flow cytometry as described above. Data were analyzed using DAKO Summit v4.3 software (Dako Cytomation, Cambridge, United Kingdom).

Characterization of Tumor-Infiltrating pDCs

Five days after the treatment with Ad.TK/GCV + Ad.Flt3L tumor-infiltrating pDCs were collected by Percoll gradient as described above, followed by staining with mouse antirat CD3-FITC, mouse antirat CD4-PeCy5, and mouse antirat CD45R-PE (see above) and purification by fluorescent-assisted cell sorting using an Ario Cell Sorter (Dako Cytomation). $CD3^-/CD45R^+/CD4^+$ cells were then characterized as follows:

Expression of activation markers. We assessed the expression of activation markers in tumor-infiltrating pDCs by flow cytometry using mouse antirat CD86 and mouse antirat MHC II–FITC (catalog nos. 555018 and 554928; BD Pharmingen). Spleen pDCs activated with 50 μg/ml ODN CpG_{2216} (catalog no. ALX-746-005; Axxora LLC, San Diego, CA) for 24 hours were used as positive control.

MHC II immunofluorescence. After 24 hours of incubation with 50 μg/ml ODN, CpG_{2216} tumor-infiltrating pDCs were fixed with 4% PFA for 20 minutes on ice. Cells were stained with mouse antirat MHC II (catalog no. MCA46GA; Serotec). Cytoskeleton was stained with phalloidin–Alexa 594 (1:200, catalog no. A12381; Molecular Probes) for 20 minutes at room temperature. Nuclei were stained with 4′, 6-diamidino-2-phenylindole (DAPI, 5 μg/ml, catalog no. D21490; Invitrogen Molecular Probes). Cells were loaded onto rounded coverslips, dried at room temperature for 24 hours and mounted with ProLong Antifade (Invitrogen Molecular Probes). We determined the percentage of pDCs containing beads by microscopy. We used spleen pDCs incubated 24 hours with ODN CpG_{2216} as positive control.

ELISA. Levels of interleukin 6 (IL-6) and tumor necrosis factor α (TNF-α) in conditioned media from tumor-infiltrating pDCs incubated with 50 μg/ml CpG_{2216} for 24 hours were determined by ELISA following the manufacturer's protocol (catalog no. ER2IL6 [Endogen Searchlight, Boston, MA] and catalog no. 88-7340 [eBiosciences, San Diego, CA], respectively). Absorbance was read on a 96-well plate reader (SpectraMax Plus; Molecular Devices, Sunnyvale, CA) at 450 and 570 nm to subtract background. Spleen pDCs incubated for 24 hours with ODN CpG_{2216} were used as a positive control.

Biologic assay for IFN-α detection. IFN-α content was assessed in serum collected from naive rats 7 days after intracranial injection

of Ad.IFN-α, in conditioned medium from activated tumor-infiltrating pDCs and in conditioned medium from COS7 cells that were infected with Ad.IFN-α (200 pfu/cell) alone or in combination with Ad.B18R (100 infectious units/cell) for 48 hours. To perform IFN-α detection CNS-1 cells were transfected with 40 ng of an interferon-sensitive response element (pISRE) linked to firefly luciferase (Clontech, Mountain View, CA) and 4 ng of constitutive expressed renilla luciferase (as internal control). After 24 hours, transfected CNS-1 cells were incubated in the presence of recombinant IFN-α (1000 U/ml, positive control, catalog no. 13100-1; R&D Systems, Minneapolis, MN), serum or conditioned medium for 6 hours. Firefly and renilla luciferase were detected using the Dual Luciferase Reporter Assay system (Promega) and a Veritas luminometer (Turner Biosystems, Sunnyvale, CA) per the manufacturer's instructions.

T-cell priming (mixed leukocyte reaction). Five days after the treatment with Ad.TK/GCV + Ad.Flt3L, tumor-infiltrating pDCs were purified from 20 rats as described above. T cells were concurrently purified from the spleen of allogeneic-naive C57/BL6 mouse by magnetic activated cell sorting after labeling with CD4 and CD8 magnetic beads (Miltenyi Biotec, Bergisch-Gladbach, Germany) as previously described [17]. Purified T cells were labeled with 5 μM CFDA-SE (Molecular Probes) per the manufacturer's instructions. A total of 20,000 labeled mouse T cells were incubated with increasing numbers of unlabeled tumor-infiltrating pDCs (0 to 20,000). Cells were incubated in X-Vivo 10 media (Cambrex, Walkersville, MD) for 5 days and subsequently analyzed by flow cytometry gating mouse T cells with a specific antimouse CD45 antibody (R&D Systems).

Bead Uptake In Vivo

Two and five days after the administration of beads, brains and cervical lymph nodes were collected and postfixed for 72 hours. Brains were sectioned with a vibratome into 60-μm serial coronal sections. The lymph nodes were cryoprotected for 24 hours in a phosphate-buffered 20% sucrose solution, frozen in Tissue-Tek OCT compound on dry ice, and sectioned with a cryostat into 30-μm sections. Immunofluorescence staining was performed as previously described [14,34] on the brain and lymph node sections. Macrophages and activated microglia were identified by mouse antirat CD68 (1:500; MCA341R; Serotec) and rabbit antirat Iba-1 (1:500; 019-19741; WAKO, Osaka, Japan). pDCs were identified by monoclonal antibodies against CD45R (1:100; IgG_{2b}, 554879; BD Biosciences) and CD4 (1:100; IgG_{2a}, 550296; BD). cDCs were identified by mouse antirat DC antibody OX-62 (1:100, 555010; BD). Alexa Fluor secondary antibodies (1:1000; Molecular Probes) were used: goat antimouse IgG 594 (A11032), goat antirabbit IgG 647 (A21245), goat antimouse IgG_{2a} 594 (A21135), and goat antimouse IgG_{2b} 647 (A21242). Nuclei were stained with DAPI (5 μg/ml; Invitrogen Molecular Probes); cells and tissues were mounted with ProLong Antifade (Invitrogen Molecular Probes). Confocal micrographs were obtained using a Leica confocal microscope TCS SP2 with AOBS equipped with 405-nm violet-diode UV laser, 488-nm argon laser, and 594- and 633-nm helium-neon lasers and using a HCX PL APO 63× 1.4 numerical aperture oil objective (Leica Microsystems Heidelberg, Mannheim, Germany).

Neuropathology

Neuropathologic analysis was performed in the brain of rats that underwent tumor regression and in naive rat brain 7 and 60 days after injecting Ad.IFN-α alone or in combination with Ad.TK. After perfusion with Tyrode solution and 4% PFA, brains were fixed in 4% paraformaldehyde for three additional days. Sixty-micrometer serial coronal sections were cut through the striatum, and free-floating immunocytochemistry was performed as previously described [14]. Briefly, endogenous peroxidases were inactivated with 0.3% hydrogen peroxide, followed by blocking in 10% horse serum/PBS. Sections were incubated for 72 hours with the following antibodies: anti–tyrosine hydroxylase (TH) in rabbit (1:5000, no. 657012; Calbiochem, La Jolla, CA), anti–myelin basic protein (MBP) in mouse (1:1000, no. MAB1580; Chemicon, Temecula, CA), antirat CD68 in mouse (clone ED1 to identify macrophages/activated microglia; 1:1000, no. MCA341R; Serotec), antirat major histocompatibility complex II (MHC II, 1:1,000, no. MCA46GA; Serotec), and antirat CD8α (to identify cytotoxic T cells; 1:1000, no. MCA48G; Serotec). Then, the sections were incubated for 4 hours with biotin-conjugated antirabbit goat IgG or antimouse rabbit IgG (1:800, nos. E0432 and E0464, respectively; DAKO, Glostrup, Denmark). Binding of biotinylated secondary antibodies was detected using the Vectastain Elite ABC horseradish peroxidase method (Vector Laboratories, Burlingame, CA) followed by the glucose oxidase and nickel ammonium sulfate–intensified diaminobenzidine method. Sections were mounted on gelatinized glass slides and dehydrated through graded ethanol solutions and coverslipped using DPX mounting medium for histology (Sigma, St Louis, MO).

Nissl staining was used to determine the histopathologic features of the brains. Briefly, brain sections were mounted on gelatinized glass slides and incubated in cresyl violet (0.1%; Sigma). Sections were passed through destain solution (70% ethanol, 10% acetic acid), dehydrated (100% ethanol and xylene), and coverslipped using DPX mounting medium for histology.

Tissues were photographed with Carl Zeiss Optical Axioplan microscope using AxioVision Rel 4.6 and MOSAIX software (Carl Zeiss, Chester, VA).

Statistical Analysis

Sample sizes were calculated to detect differences between groups with a power of 80% at a 0.05 significance level using PASS 2008 (Power and sample size software; NCSS, Kaysville, UT). Kaplan-Meier survival curves were analyzed using the Mantel log rank (GraphPad Prism version 3.00; GraphPad Software, San Diego, CA). Flow cytometry, phagocytosis, and ELISA data were analyzed by analysis of variance (ANOVA; NCSS). When data failed normality or Levene test for variance homogeneity, they were log transformed. Randomization test was used to analyze body weight curves (NCSS). $P < .05$ was used to determine the null hypothesis to be invalid. The statistical tests used are indicated in the figure legends.

Results

Recruitment of Tumor-Infiltrating Immune Cells into the Tumor Microenvironment in Response to Intratumoral Expression of TK and Flt3L in a Syngeneic, Orthotopic Rat GBM Model

Our previous results showed that intratumoral administration of Ad.TK + Ad.Flt3L triggers an antitumor immune response that leads to tumor regression and long-term survival in ~70% of rats bearing intracranial syngeneic GBM [14,19,35]. In the present work, we aimed to identify which immune cells are recruited within the tumor microenvironment in response to this therapeutic approach. Lewis rats were implanted in the brain with syngeneic CNS-1 cells, and 10 days later, they were treated with an intratumoral injection of Ad.TK + Ad.Flt3L,

saline, or an empty Ad (Ad.0), as controls. At 5 and 12 days after the treatment, mononuclear cells were purified from the tumors and analyzed by flow cytometry (Figure 1). We found that treatment with Ad.TK + Ad.Flt3L induced recruitment of APCs into the brain tumor mass. Although macrophages and cDCs were readily detected within the tumor of control rats, treatment with Ad.TK + Ad.Flt3L increased approximately three-fold the infiltration levels of these cells into the tumor microenvironment. However, pDCs were found only in the brain tumor of Ad.TK + Ad.Flt3L-treated rats and were virtually absent in control animals treated with saline or Ad.0. The levels of microglial cells remained unchanged after treatment with saline, Ad.0, or Ad.TK + Ad.Flt3L at both time points. We also observed that NK cells were increased three-fold in the tumor mass 5 days after treatment with Ad.TK + Ad.Flt3L. B lymphocytes were virtually absent in the tumor of control-treated rats and were recruited into the tumor microenvironment in response to the combined gene therapy 12 days after the treatment. T cells were elevated in the tumors treated with Ad.0 and Ad.TK + Ad.Flt3L, when compared with saline-treated control rats.

Tumor-Infiltrating pDCs Exhibit an Immature Phenotype and Are Capable of T-cell Priming

The role of pDCs in brain tumor immunology remains debated [23,36]. Also, it is not clear whether these cells play a role in the process of antigen uptake and presentation during the onset of immune responses or they only act as IFN type I–producing cells [27]. We characterized tumor-infiltrating pDCs recruited in response to Ad.TK + Ad. Flt3L treatment. Five days after treatment, immune cells were collected and pooled from the tumors (n = 25), and pDCs were purified by FACS ($CD3^-/CD45R^+/CD4^+$; Figure 2*A*). To determine the activation status of tumor-infiltrating pDCs, we assessed the expression levels of activation markers, their capability of releasing cytokines, as well as their ability to become activated in response to TLR9 agonist CpG_{2216}. The levels of expression of MHC II and CD86 were determined by flow cytometry, using spleen pDCs activated with CpG_{2216} as positive controls. We found that tumor-infiltrating pDCs expressed very low levels MHC II and CD86, when compared with activated spleen pDCs (Figure 2*B*), suggesting that pDCs within the brain tumor microenvironment exhibit an immature phenotype. Tumor pDCs were then activated *in vitro* by incubating with TLR9 agonist CpG_{2216} for 24 hours. Cytokine release was assessed by ELISA (Figure 2*C*), and expression of MHC II was assessed by immunostaining (Figure 2*D*), using spleen pDCs as positive controls. We found that tumor pDCs can be readily activated *in vitro* by Cpg_{2216}, releasing large amounts of IFN-α (Figure 2*C*) and upregulating MHC II expression (Figure 2*D*). Incubation with CpG_{2216} also increased the release of TNF-α and IL-6 from pDCs *in vitro* (Figure 2*C*).

We next aimed to assess whether tumor-infiltrating pDCs recruited on Ad.TK + Ad.Flt3L treatment exhibited phagocytic activity within the brain tumor microenvironment. The phagocytic activity of tumor-infiltrating pDCs was evaluated *in vivo* in tumor-bearing rats treated with Ad.TK/GCV + Ad.Flt3L using yellow-green beads that were injected intratumorally 3 days after the treatment (Figure 3*A*). Our results indicate that the beads were distributed throughout the brain tumor mass (Figure W1*A*). Beads were detected in the cytoplasm of tumor-infiltrating $OX\text{-}62^+$ cells (Figure 3*B*) and $CD45R^+/CD4^+$ cells (Figure 3*C*), suggesting that both cDCs and pDCs exhibit phagocytic activity. Macrophages containing beads were also readily found in the brain tumor microenvironment (Figure W1*B*). Cells containing beads were also detected in the cervical lymph nodes, some of which expressed CD45R and CD4, which are markers for pDCs (Figure 3*D*), suggesting that they are capable of trafficking to the dLNs where they could interact with naive T cells.

To assess whether tumor-infiltrating pDCs were able to prime T cells, we performed an allogeneic mixed leukocyte reaction. Tumor-infiltrating pDCs were collected from the brain 5 days after the treatment with Ad.TK/GCV + Ad.Flt3L and incubated with T cells purified from the spleen of allogeneic C57/BL6 mice and labeled with CFDA-SE (Figure 4*A*). T-cell proliferation was determined by flow cytometry as the decay in CFDA-SE fluorescence. We found that increasing concentrations of tumor-infiltrating pDCs stimulated the proliferation of allogeneic T cells, suggesting that tumor-infiltrating pDCs are capable of providing costimulatory signals that are required to support T-cell proliferation.

pDCs Delivered into the Tumor Microenvironment Mimic the Effect of Ad.Flt3L

Because we found that tumor-infiltrating pDCs were capable of phagocytosis and T-cell priming, we next aimed to establish the relevance of tumor-infiltrating pDCs in triggering the antitumor immune response induced by Ad.TK + Ad.Flt3L. Therefore, we tested the hypothesis that pDCs would mimic the effect of Ad.Flt3L when administered intratumorally in combination with Ad.TK. To obtain adequate numbers of pDCs for this experiment, naive rats were injected intravenously with Ad.Flt3L, which expands the pDC population in the bone marrow (from <0.5% to 3.5% of bone marrow leukocytes; not shown). Two weeks later, bone marrow pDCs were purified by FACS ($CD3^-/CD4^+/CD45R^+$; Figure 4*B*) and incubated in the presence of CNS-1 cell lysates. These pulsed pDCs (150,000/rat) were mixed with CpG 2216 immediately before intratumoral injection on day 10 after tumor implantation. To avoid the infection of pDCs with Ad.TK, rats received the injection of Ad.TK 24 hours before treatment with pDCs (day 9 after tumor implantation). Whereas all the rats that received Ad.TK or pDCs alone died because of tumor burden, combined therapy with Ad.TK + pDCs led to tumor regression and long-term survival in 35% of the rats (Figure 4*C*). These findings suggest that pDCs play an important role in mediating the antitumor immune response induced by Ad.TK + Ad.Flt3L.

IFN-α Mediates the Therapeutic Effect of Ad.TK + Ad.Flt3L

Considering that the main cytokine secreted by pDCs is IFN-α, we next aimed to elucidate whether the therapeutic efficacy of Ad.TK + Ad.Flt3L was dependent on IFN-α. We constructed an Ad encoding B16R (Ad.B18R), a type I interferon-binding protein that blocks IFN-α function [31], under the control of the ubiquitous murine CMV promoter (Figure W2). We first assessed the ability of Ad.B18R to block the function of IFN-α *in vitro* (Figure 5*A*). COS7 cells were infected with a vector expressing IFN-α (Ad.IFN-α) in the presence or absence of increasing concentrations of Ad.B18R, and IFN-α levels were assessed by a biologic assay using the pISRE plasmid, which encodes an interferon-sensitive response element linked to firefly luciferase. A plasmid encoding constitutive renilla luciferase was used as internal control. We found that expression of B18R blocks the function of IFN-α in a dose-dependent manner, and thus we used Ad.B18R to block the activity of IFN-α *in vivo*. Ten days after tumor implantation, rats received an intratumoral injection of saline or Ad.TK + Ad.Flt3L alone or in combination with Ad.B18R (Figure 5*B*). Treatment with Ad.B18R led to complete failure of the immune therapy, suggesting that the release of IFN-α is crucial to establish the antitumor immune response triggered by Ad.TK + Ad.Flt3L.

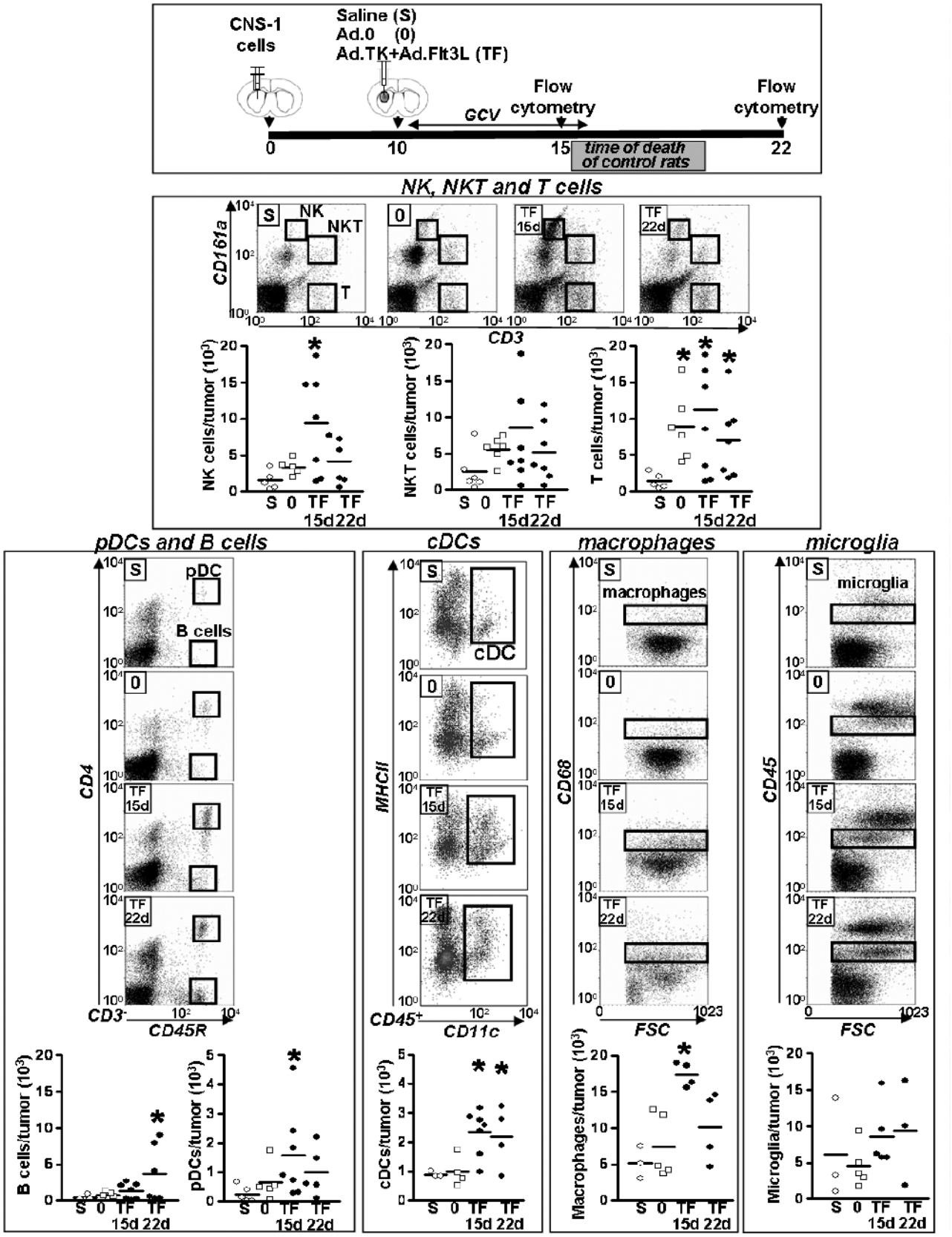

Figure 1. Quantification of tumor-infiltrating immune cells. A total of 5000 CNS-1 cells were implanted in the striatum of Lewis rats, and 10 days later, rats received an intratumoral injection of Ad.Flt3L + Ad.TK followed by daily administration of GCV or, as controls, saline or an empty vector (Ad.0). At 5 and 12 days after the treatment, brain mononuclear cells were isolated from the brain tumors and analyzed using flow cytometry. Note that because control rats die of tumor burden at days 17 to 20, they cannot be included in day 22 analysis. *$P < .05$ *versus* saline. Kruskal-Wallis test followed by Dunn test.

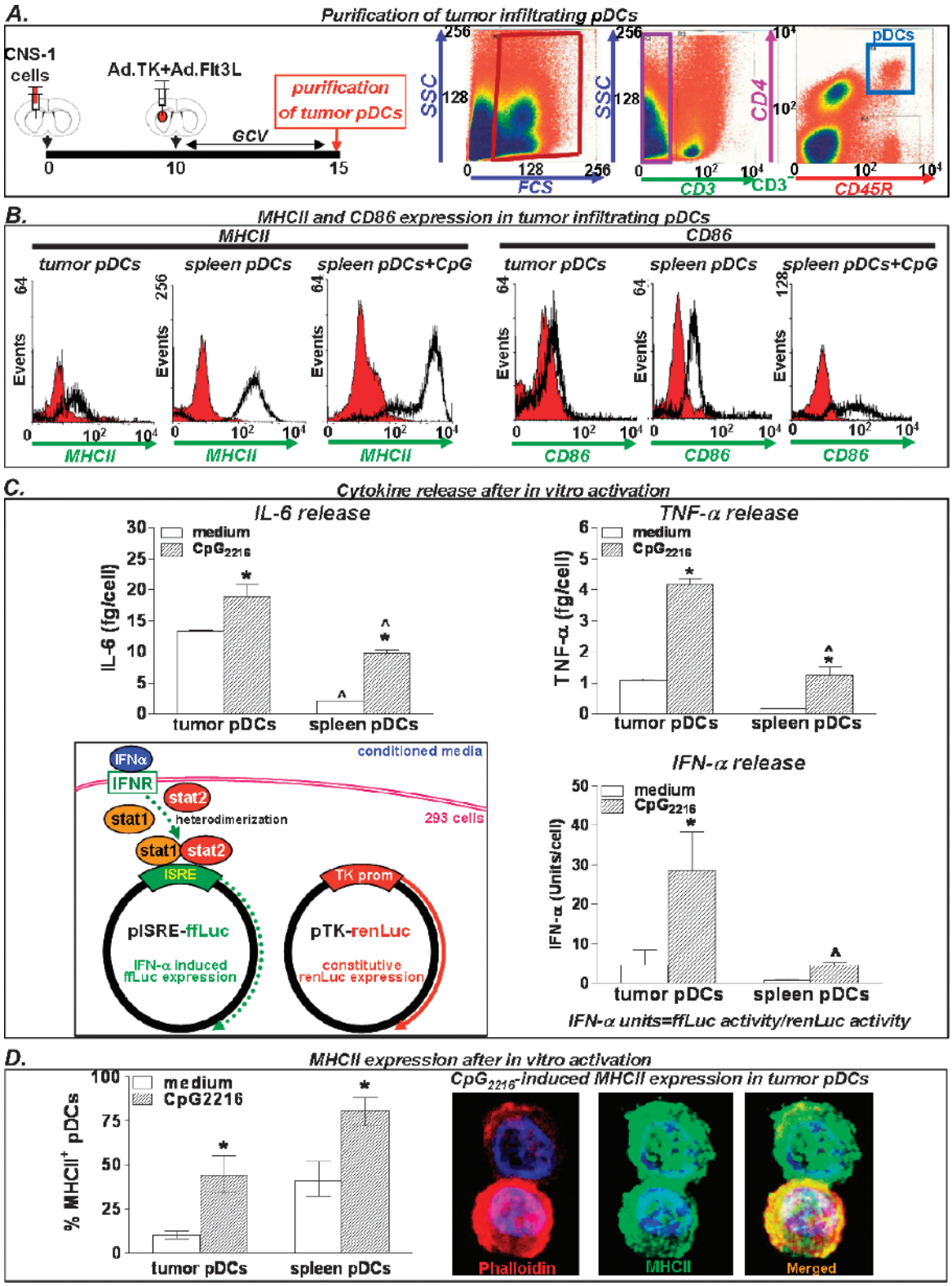

Figure 2. Activation markers and cytokine release in tumor-infiltrating pDCs. (A) Immune cells from CNS-1 tumors were collected 5 days after treatment with Ad.TK + Ad.Flt3L and $CD3^{-}CD45R^{+}CD4^{+}$ cells were purified by flow cytometric cell sorting. Cells were characterized by expression of activation markers and cytokine release. (B) Expression of activation markers CD86 and MHC II was determined by flow cytometry. Naive spleen pDCs incubated 24 hours with ODN CpG_{2216} were used as positive controls. (C) Cytokine release was determined in tumor-infiltrating pDCs and naive spleen pDCs after incubation with ODN CpG_{2216} for 24 hours. IL-6 and TNF-α expressions were detected by ELISA, and IFN-α expression was assessed by a biologic assay using the pISRE plasmid. $*P < .05$ *versus* medium; $\hat{}P < .05$ *versus* tumor pDCs. Two-way ANOVA followed by Student-Newman-Keuls test. (D) Columns represent the percentage of pDCs expressing MHC II, as determined by immunofluorescence, after incubation with ODN CpG 2216 for 24 hours. Pictures in the right show ODN CpG_{2216}-induced MHC II expression in tumor-infiltrating pDCs (green). Cytoskeleton was stained with phalloidin–Alexa 594 (red). Nuclei were stained with DAPI.

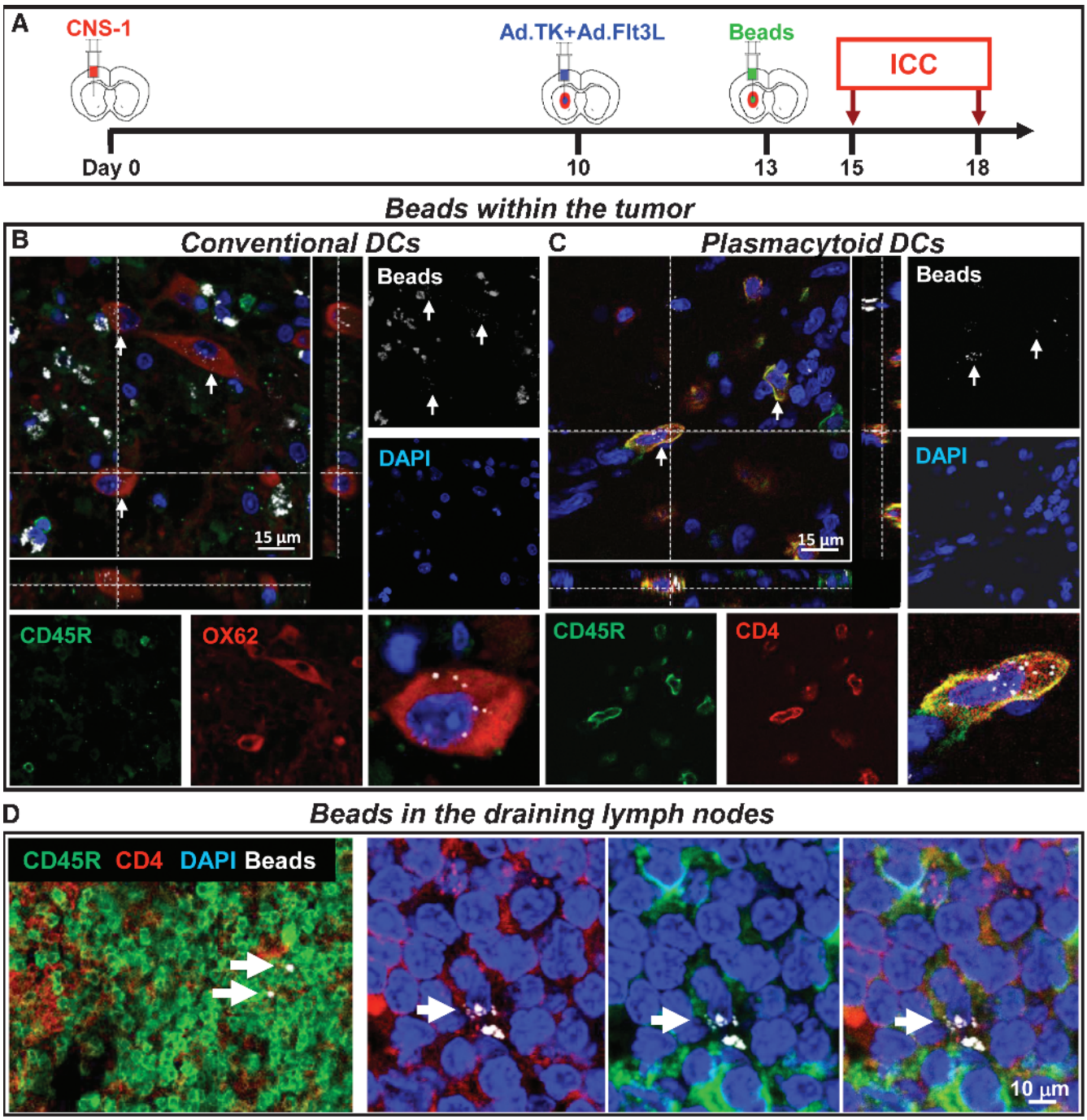

Figure 3. Phagocytic activity by cDCs and pDCs. (A) Three days after treatment with Ad.TK + Ad.Flt3L tumor-bearing rats were injected intratumorally with fluorescent microbeads. Two days later, the brains immune cells were detected by immunofluorescence. Bar, 15 μm. (B) Confocal microphotograph showing tumor-infiltrating cells expressing the cDC marker OX62 (red) containing beads (white) in the cytoplasm (indicated by arrows). (C) Confocal microphotograph showing tumor-infiltrating cells expressing the pDC markers CD45R (green) and CD4 (red) and containing beads (white) in the cytoplasm (indicated by arrows). (C) Confocal microphotograph showing cells in the cervical lymph nodes expressing the pDC markers CD45R (green) and CD4 (red) and containing beads (white) in the cytoplasm (indicated by arrows). Nuclei were stained with DAPI (blue). Bar, 10 μm.

In view of the central role of IFN-α in the antitumor immunity triggered by Ad.TK + Ad.Flt3L, we evaluated whether a vector encoding IFN-α could also trigger antitumor immunity in this model. We first assessed the efficacy of Ad.IFN-α in rats bearing small intracranial CNS-1 tumors. We found that intratumoral administration of Ad.IFN-α 4 days after tumor implantation led to long-term survival in more than 50% of rats (Figure W3). However, when we treated rats bearing larger tumors (day 10 after tumor implantation), we found that Ad.IFN-α alone did not induce tumor regression (Figure 5*C*). Conversely, when rats bearing large tumors were treated with a combination of Ad.IFN-α and Ad.TK, more than 50% exhibited tumor regression and long-term survival (Figure 5, *C* and *D*). Taken together, these findings indicate that IFN-α plays a critical role in Ad.TK/Ad/Flt3L mediated anti-GBM therapeutic efficacy.

Expression of IFN-α in the Normal Brain Parenchyma Leads to Overt Toxicity

Considering that in the clinical scenario, gene therapy vectors are injected into the tumor bed after surgical resection, it was important to determine any putative toxicity toward the normal brain parenchyma. Thus, we next assessed the safety of Ad.IFN-α alone or in combination with Ad.TK in the brain of naive rats and compared it with Ad.Flt3L + Ad.TK. Control rats received saline or Ad.0. Neuropathology was assessed 7 and 60 days later. We found that controls and rats that received Ad.TK alone did not exhibit signs of local toxicity. Tallying with our previous results [14], injection of Ad.TK + Ad.Flt3L into the naive rat brain did not affect the integrity of the brain and did not lead to overt inflammation. We observed only a mild and transient infiltration of inflammatory cells, similar to that induced by injection of Ad.0. In contrast, rats that received Ad.IFN-α alone or in combination with Ad.TK exhibited signs of severe local toxicity 7 days after the treatment, including hemorrhages, necrosis, demyelinization, and inflammation with profuse infiltration of immune cells (Figures 6 and W4). These signs of neurotoxicity were irreversible with severe ventriculomegaly and chronic local inflammation that were still evident 60 days after

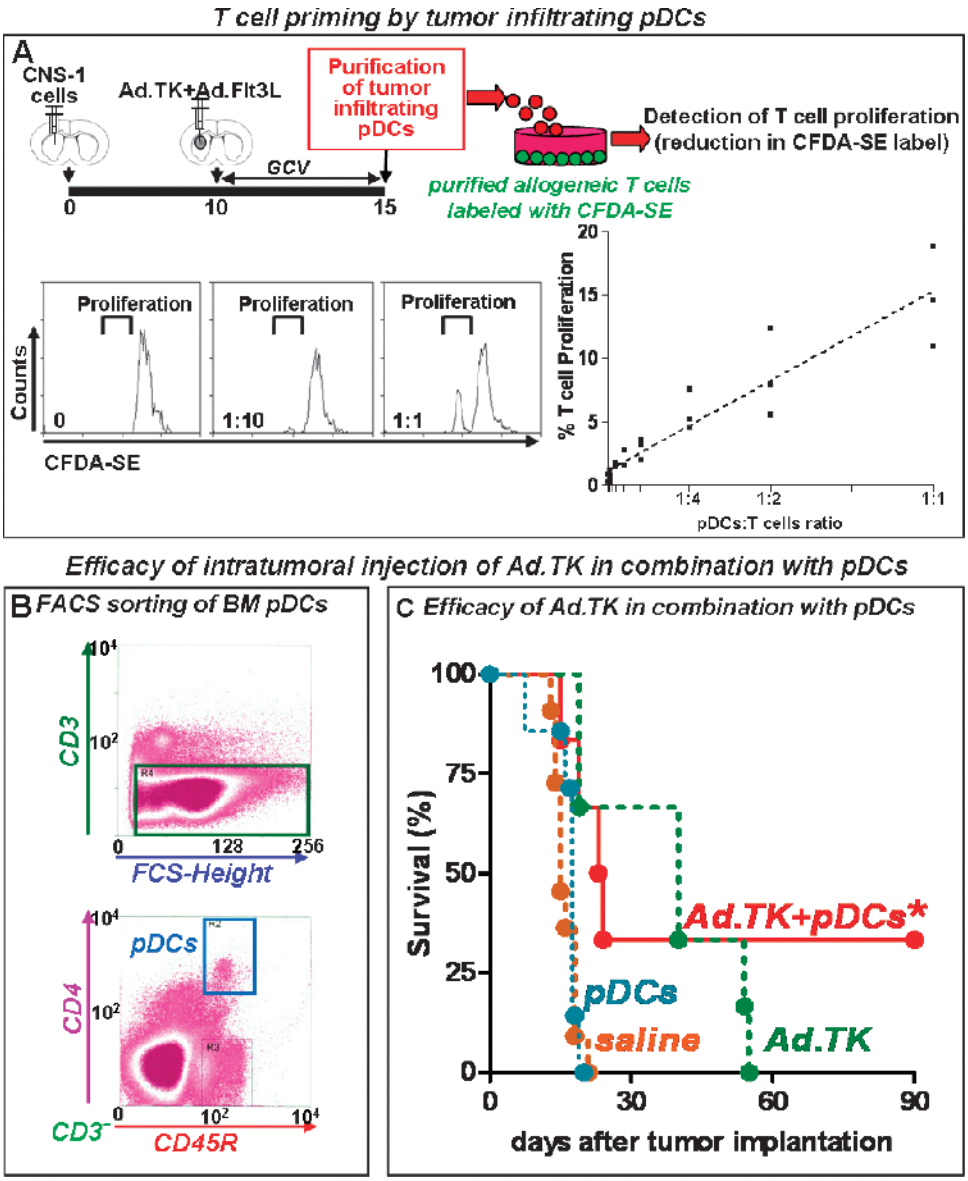

Figure 4. pDCs are able to prime T cells and eradicate intracranial GBM. (A) Tumor-infiltrating pDCs were purified by FACS ($CD3^-$, $CD45R^+$, $CD4^+$) 5 days after the treatment with Ad.TK/GCV + Ad.Flt3L. The ability of tumor-infiltrating pDCs to stimulate T-cell proliferation was assessed by an allogeneic mixed leukocyte reaction. Increasing concentrations of tumor-infiltrating pDCs (stimulators) were incubated with 20,000 CFDA-SE–labeled T cells (responders) collected from the spleen of allogeneic C57/BL6 mice. T-cell proliferation was determined by the reduction in CFDA-SE fluorescence, as assessed by FACS. Representative histograms show CFDA-SE–labeled T cells incubated with increasing ratios of pDCs. (B) pDCs from the bone marrow of rats that were intravenously injected with Ad.Flt3L 14 days before were purified by FACS ($CD3^-/CD4^+/CD45R^+$). Dot plots show the gates for cell collection. pDCs were then incubated in the presence of CNS-1 cell debris (debris/pDCs ratio was 3:1) followed by activation with CpG 2216. (C) Kaplan-Meier curves showing the survival of tumor-bearing rats treated with Ad.TK at day 8 after tumor implantation, followed by intratumoral injection of activated pDCs 24 hours later. Rats received GCV for 7 days. *$P < .05$ *versus* saline. Log-rank test.

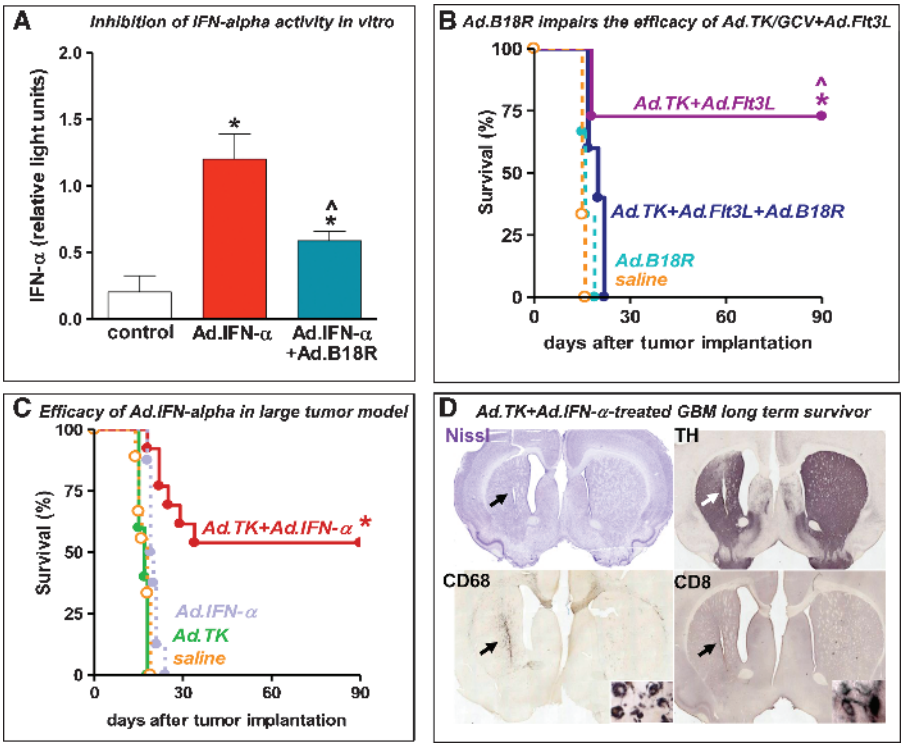

Figure 5. Role of IFN-α in mediating the efficacy of immunotherapy in rat intracranial GBM. (A) COS7 cells were infected with a vector expressing IFN-α (Ad.IFN-α) in the presence or absence of Ad.B18R (100 infectious units [iu]/cell), an Ad vector encoding the neutralizing type I interferon receptor B18R, which blocks endogenous IFN-α. IFN-α function was assessed by a biologic assay using the pISRE plasmid. *$P < .05$ *versus* uninfected cells (white column); ^$P < .05$ *versus* Ad.IFN-α without Ad.B18R (red column). One-way ANOVA followed by Student-Newman-Keuls test. (B) Ten days after tumor implantation, rats received intratumoral injections of saline or Ad.TK + Ad.Flt3L alone or in combination with AdB18R, followed by daily administration of GCV for 7 days. *$P < .05$ *versus* saline; ^$P < .05$ *versus* Ad.TK + Ad.Flt3L + Ad-B18R. Mantel log-rank test. (C) Tumor-bearing rats were treated 9 days after tumor implantation by intratumoral injection of saline or Ad.IFN-α alone or in combination with Ad.TK followed by daily GCV administration. *$P < .05$ *versus* saline. Mantel log-rank test. (D) Images showing the neuropathology of a representative Ad.TK + Ad.IFN-α–treated survivor, as assessed by Nissl staining and immunocytochemistry of TH, CD68 (macrophages/activated microglia), and CD8α (T cells). Arrows indicate the scar left after tumor regression.

injection (Figure W5). Our findings suggest that, whereas intracranial administration of Ad.TK + Ad.Flt3L in the brain is safe, administration of Ad.IFN-α poses risks of neurotoxicity. Because IFN-α was readily detected in the serum of the rats that received intracranial injections of Ad.IFN-α (Figure 7*A*), we assessed whether they also exhibited signs of systemic toxicity. Rats that received Ad.IFN-α alone or in combination with Ad.TK underwent an acute weight loss, which was more pronounced 5 days after injection (Figure 7*B*).

Discussion

We previously observed that Flt3L recruits pDCs into the naive brain parenchyma [22]. Considering that the role of pDCs in tumor immunology remains debated [23], we aimed to assess the role played by pDCs in the antitumor immune response elicited by Ad.TK/GCV + Ad.Flt3L. We found that the administration of Ad.TK/GCV + Ad.Flt3L induced active recruitment of plasmacytoid DCs (pDCs) into the brain tumor microenvironment, which were capable of *in vivo* phagocytosis, IFN-α release, and T-cell priming. Whereas the presence of pDCs has been observed in several types of solid tumors, including head and neck cancer, ovarian cancer, and melanoma [37], pDCs seem to be absent within the tumor mass of patients with GBM [38]. Tallying with this, we did not observe pDCs in untreated CNS-1 GBM. Other populations of APCs were readily detected in CNS-1 tumors, including macrophages and cDCs. The profile of APC infiltration in CNS-1 tumors was similar to that reported for human GBM [38]. Although there is a predominance of microglia/macrophages followed by cDCs in freshly isolated human glioma specimens, very few pDCs can be detected [38]. A reduction in the levels of circulating pDCs has also been reported in patients with different types of malignant tumors, including GBM [39]. Levels of pDCs are reduced in the blood of patients with GBM, prostate, and breast cancer when compared to healthy donors, and there is a significant increase of circulating immature $CD11c^+$ cells that exhibit poor APC capability and correlate with tumor growth [39].

We found that administration of Ad.TK + Ad.Flt3L induced a fast increase in the infiltration of all APC populations in the brain tumor mass, which could promote tumor antigen presentation. Because pDCs were detected in the tumor mass only when rats were treated with Ad.TK + Ad.Flt3L, they secrete high levels of IFN-α and are capable of T-cell priming, we hypothesized that they could be playing an important role in the antitumor immune response induced by this treatment [14,19,35,40,41]. It has been proposed that cDCs and pDCs that accumulate in solid tumors are tolerogenic [42,43] and have a diminished capacity to respond to inflammatory stimuli like TLR9 agonist CpG [37]. However, pDCs isolated from human tumor specimens exhibit the ability to uptake antigen, migrate, and produce proinflammatory cytokines, namely, IL-12 and IFN-α, and their activation using TLR agonists

seems to have clinical value in cancer patients [44]. Here we observed that glioma-infiltrating pDCs produced higher levels of inflammatory cytokines on activation with CpG than did naive spleen pDCs. CpG activation also induced the expression of MHC II in tumor-infiltrating pDCs, as well as in naive spleen pDCs. These findings indicate that tumor-infiltrating pDCs recruited by Ad.TK + Ad.Flt3L treatment have an intact response to TLR9 activation. Although the expression of activation markers was relatively low in tumor-infiltrating pDCs, we showed that these cells exhibit phagocytic activity and are capable of T-cell priming. These findings indicate that tumor-infiltrating pDCs could play a role as APCs in the antitumor immune response induced by Ad.TK + Ad.Flt3L treatment.

It has been reported that tumor cells can inhibit pDC function through the release of anti-inflammatory cytokines such as tumor growth factor β, vascular endothelial growth factor, and IL-10 into the tumor microenvironment, which would reduce the ability of tumor-infiltrating pDCs to trigger antitumor immunity [37,44]. However, when we delivered tumor lysate–loaded pDCs activated with CpG into the CNS-1 tumors treated with Ad.TK, they elicited tumor regression in 35% of the rats, whereas all the rats treated with Ad.TK alone died to tumor burden. Although the pDCs used in our experiment were obtained from the bone marrow of rats injected intravenously with Ad.Flt3L, the immune response triggered seems to be tumor antigen specific rather than against putative Ad antigens presented by pDCs. We have not assessed the possibility of Ad infection in the pDC population; however, it is unlikely that Ad antigens trigger an immune response that eradicates tumor cells. If the immune response were against Ad antigens presented by pDCs, it would lead to the destruction of pDCs, preventing antitumor efficacy. Also, administration of pDCs without treating the tumor with Ad.TK did not induce tumor regression or improved survival because the rats died of tumor burden at the same time that saline-treated control rats did. Further, in previous publications, we did not detect evidence of anti-Ad immunity in Ad-treated tumor-bearing animals [45], which indicates that intracranial administration of these vectors does not stimulate an anti-Ad immune response. Our findings agree with previous reports that show that TLR9-activated pDCs can trigger an antitumor immune response that involves the sequential activation of NK cells, cDCs, and CD8 T cells and leads to the regression of experimental

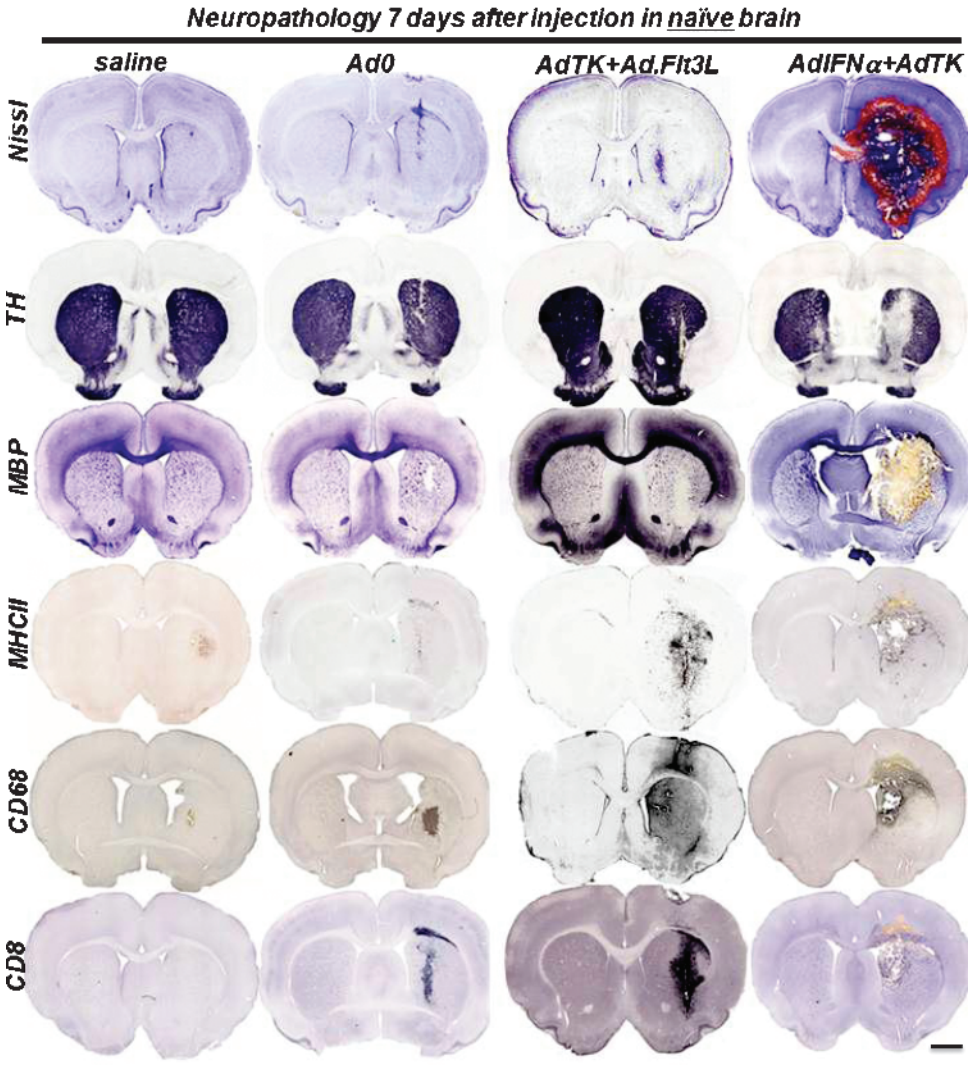

Figure 6. Acute neurotoxicity after Ad.IFN-α injection in naive rat brain. Naive Lewis rats were injected with Ad.IFN-α or Ad.Flt3L in the striatum in combination with Ad.TK. As controls, rats received saline or Ad.0. Rats treated with Ad.TK received GCV treatment daily. Seven days after vector delivery, neuropathologic analysis of the brain was assessed by Nissl staining and immunocytochemistry using antibodies against TH, MBP, MHC II, CD68 (macrophages/activated microglia), and CD8α (T cells). Scale bar, 2 mm.

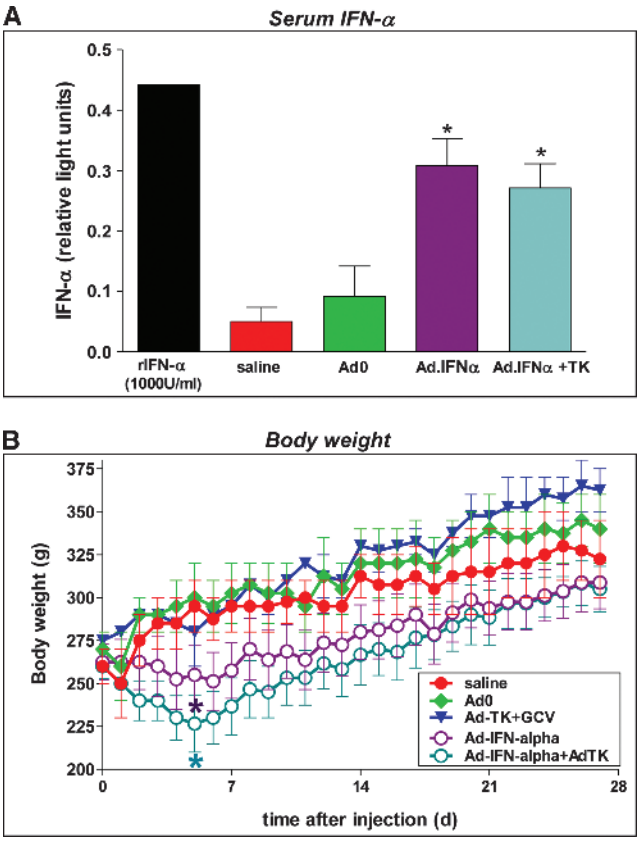

Figure 7. Weight loss after Ad.IFN-α injection in naive rat brain. (A) Circulating levels of IFN-α were assessed by a biologic assay using the pISRE plasmid in serum collected 7 days after Ad administration. Recombinant rat IFN-α (rIFN-α, 1000 U/ml) was used as positive control. *$P < .05$ *versus* saline. One-way ANOVA followed by Student-Newman-Keuls test. (B) Body weight was assessed daily in a group of rats for 4 weeks. *$P < .05$ *versus* saline. Randomization test.

melanomas in mice [46]. It is possible that pDCs recruited into the brain tumor mass upon treatment with Ad.TK + Ad.Flt3L undergo activation in response to intracellular proinflammatory molecules released by dying tumor cells [17]. We have previously shown that the efficacy of this treatment is dependent on the release from tumor cells undergoing cell death [14,17], of the DNA binding protein, high-mobility group box 1 (HMGB1), which acts as an endogenous TLR agonist [47,48]. HMGB1 activates TLR2 in cDCs [17]. Tallying with our findings using pDCs (Figure 4*C*), intratumor administration of cDCs leads to eradication of intracranial GBM in approximately 40% of tumor-bearing animals [17], suggesting that both subtypes of DCs participate in antitumor immunity induced by Ad-TK + Ad.Flt3L.

It has been previously shown that pDCs activation is required for T-cell priming and is characterized by the up-regulation of co-stimulatory molecules and the release of proinflammatory molecules, such as IL-6, TNF-α, and IFN-α [49]. IFN-α released from pDCs is an important immune mediator because it regulates the activation of other immune cells, such as cDCs, NK cells, and T cells [27], and shows direct antitumor and antiangiogenic activity [6]. Tumor-infiltrating pDCs released high levels of basal and CpG-induced IFN-α, which could be involved in the antitumor immune response induced by our treatment. Indeed, our results using the IFN-α decoy receptor B18R show that the efficacy of Ad.TK + Ad.Flt3L is dependent on the release of IFN-α. This cytokine exhibits a robust direct antitumor effect by inhibiting angiogenesis and tumor cell proliferation and also stimulates the immune system to target and eradicate tumor cells [6]. In our model, intratumoral delivery of IFN-α in combination with Ad.TK led to the regression of established CNS-1 gliomas. These findings are in agreement with previous reports that show that Ad-mediated IFN-α delivery alone or in combination with intratumor DC vaccines leads to regression of GL261 tumors in mice [50]. However, our data demonstrated that delivery of this cytokine into the normal brain parenchyma led to considerable local and systemic toxicity. Rats that received Ad.IFN-α exhibited signs of acute neurotoxicity, such as hemorrhages, necrosis, demyelinization, and inflammation, which were irreversible, with severe ventriculomegaly and signs of chronic local inflammation still evident 2 months later. Because gene therapy vectors are injected into the tumor bed after surgical resection, the toxicity of IFN-α toward the normal brain parenchyma reduces the suitability of this cytokine for the treatment of GBM.

Alternative IFN-α delivery strategies for the treatment of GBM have been attempted using bone marrow–derived monocytes that express IFN-α [51]. Adoptive transfer of these monocytes led to regression of experimental intracranial GBM. Although because of the tumor-homing specificity of these monocytes, there were negligible systemic IFN-α expression and toxicity [51], the authors did not assess the putative neurotoxicity of the treatment, and considering that the tumors were implanted in nude mice, it was not possible to assess immune-mediated toxicities in this model. Thus, the data reported in this study highlight the significance of performing *in vivo* toxicity studies before clinical translation of powerful proinflammatory cytokines for brain tumor therapeutics. Our results indicate that, although the immune response triggered by Ad.TK + Ad.Flt3L is mediated by the release of IFN-α, the treatment does not induce apparent neurologic or systemic side effects [14]. When exogenous IFN-α is delivered into the brain, the lack of physiological regulation of its inflammatory functions leads to overt toxicity, limiting its therapeutic implementation. However, when IFN-α is released from pDCs recruited into the brain tumor by Ad.TK + Ad.Flt3L, it does not elicit local or systemic toxic effects.

Although our results indicate that pDCs participate in the antitumor effect of Ad.TK/GCV + Ad.Flt3L through the production of IFN-α, it is possible that they also play a role as APCs, priming the adaptive antitumor immune response induced by this treatment. Tumor-infiltrating pDCs supported T-cell proliferation and exhibited phagocytic activity within the tumor microenvironment. Yellow-green beads that were injected intratumorally were detected in the cytoplasm of tumor-infiltrating $CD45R^+/CD4^+$ cells *in vivo*, indicating that pDCs exhibit phagocytic activity. Cells expressing markers for pDCs were detected in the cervical lymph nodes containing beads, suggesting that they are capable of trafficking to the dLNs where they could interact with naive T cells.

In summary, we observed that pDCs recruited into the tumor mass on Ad.TK/GCV + Ad.Flt3L exhibit the ability to uptake and transport fluorescent beads present within the tumor microenvironment, produce inflammatory cytokines, and support T-cell proliferation. Our data indicate that IFN-α release by activated pDCs plays a critical role in the antitumor immunity induced by Ad.TK/GCV + Ad.Flt3L. Thus, manipulation of pDCs constitutes a novel target for the treatment of brain cancer. In this regard, the *in vitro* expansion of pDCs can be exploited in the development of antitumor vaccines [52]. pDC-based vaccines have shown strong antitumor efficacy in mouse models of cancer [53]. Importantly, these vaccines stimulate the intratumoral infiltration of antigen-specific lymphocytes in patients with melanoma [53]. The activation of immature tumor-infiltrating pDCs can also be

achieved using TLR agonists [54]. Intratumor administration of the TLR9 agonists, ODN CpGs, induces T cell–dependent antitumor immunity, reducing the size of solid tumors, namely, lymphoma and melanoma, implanted in mice [55]. Direct tumor injection of ODN CpGs stimulates the regression of malignant skin neoplasms in human patients [56]. Imiquimod, a synthetic TLR7 agonist, has also been shown to induce the accumulation of pDCs and increase the production of IFNs in skin malignancies [52]. These strategies could be useful adjuvants to further enhance the activity of glioma-infiltrating pDCs recruited by Ad.TK + Ad.Flt3L treatment.

References

[1] Hegi ME, Diserens AC, Gorlia T, Hamou MF, de Tribolet N, Weller M, Kros JM, Hainfellner JA, Mason W, Mariani L, et al. (2005). MGMT gene silencing and benefit from temozolomide in glioblastoma. *N Engl J Med* **352**, 997–1003.

[2] Lefranc F, Brotchi J, and Kiss R (2005). Possible future issues in the treatment of glioblastomas: special emphasis on cell migration and the resistance of migrating glioblastoma cells to apoptosis. *J Clin Oncol* **23**, 2411–2422.

[3] Hegi ME, Diserens AC, Godard S, Dietrich PY, Regli L, Ostermann S, Otten P, Van Melle G, de Tribolet N, and Stupp R (2004). Clinical trial substantiates the predictive value of *O*-6-methylguanine-DNA methyltransferase promoter methylation in glioblastoma patients treated with temozolomide. *Clin Cancer Res* **10**, 1871–1874.

[4] Wallner KE, Galicich JH, Krol G, Arbit E, and Malkin MG (1989). Patterns of failure following treatment for glioblastoma multiforme and anaplastic astrocytoma. *Int J Radiat Oncol Biol Phys* **16**, 1405–1409.

[5] Sgorbissa A, Tomasella A, Potu H, Manini I, and Brancolini C (2011). Type I IFNs signaling and apoptosis resistance in glioblastoma cells. *Apoptosis* **16**, 1229–1244.

[6] Borden EC, Sen GC, Uze G, Silverman RH, Ransohoff RM, Foster GR, and Stark GR (2007). Interferons at age 50: past, current and future impact on biomedicine. *Nat Rev Drug Discov* **6**, 975–990.

[7] De Bouard S, Guillamo JS, Christov C, Lefevre N, Brugieres P, Gola E, Devanz P, Indraccolo S, and Peschanski M (2003). Antiangiogenic therapy against experimental glioblastoma using genetically engineered cells producing interferon-α, angiostatin, or endostatin. *Hum Gene Ther* **14**, 883–895.

[8] Ohno S, Nishi T, Kojima Y, Haraoka J, Ito H, and Mizuguchi J (2002). Combined stimulation with interferon α and retinoic acid synergistically inhibits proliferation of the glioblastoma cell line GB12. *Neurol Res* **24**, 697–704.

[9] Tsuno T, Mejido J, Zhao T, Schmeisser H, Morrow A, and Zoon KC (2009). IRF9 is a key factor for eliciting the antiproliferative activity of IFN-α. *J Immunother* **32**, 803–816.

[10] Roth W, Wagenknecht B, Dichgans J, and Weller M (1998). Interferon-α enhances CD95L-induced apoptosis of human malignant glioma cells. *J Neuroimmunol* **87**, 121–129.

[11] Parmar S and Platanias LC (2003). Interferons: mechanisms of action and clinical applications. *Curr Opin Oncol* **15**, 431–439.

[12] Olson JJ, James CD, Lawson D, Hunter S, Tang G, and Billingsley J (2004). Correlation of the response of recurrent malignant gliomas treated with interferon α with tumor interferon α gene content. *Int J Oncol* **25**, 419–427.

[13] Candolfi M, Kroeger KM, Muhammad AK, Yagiz K, Farrokhi C, Pechnick RN, Lowenstein PR, and Castro MG (2009). Gene therapy for brain cancer: combination therapies provide enhanced efficacy and safety. *Curr Gene Ther* **9**, 409–421.

[14] Candolfi M, Yagiz K, Foulad D, Alzadeh GE, Tesarfreund M, Muhammad AK, Puntel M, Kroeger KM, Liu C, Lee S, et al. (2009). Release of HMGB1 in response to proapoptotic glioma killing strategies: efficacy and neurotoxicity. *Clin Cancer Res* **15**, 4401–4414.

[15] Muhammad AK, Puntel M, Candolfi M, Salem A, Yagiz K, Farrokhi C, Kroeger KM, Xiong W, Curtin JF, Liu C, et al. (2010). Study of the efficacy, biodistribution, and safety profile of therapeutic gutless adenovirus vectors as a prelude to a phase I clinical trial for glioblastoma. *Clin Pharmacol Ther* **88**, 204–213.

[16] Puntel M, Muhammad AK, Candolfi M, Salem A, Yagiz K, Farrokhi C, Kroeger KM, Xiong W, Curtin JF, Liu C, et al. (2010). A novel bicistronic high-capacity gutless adenovirus vector that drives constitutive expression of herpes simplex virus type 1 thymidine kinase and tet-inducible expression of Flt3L for glioma therapeutics. *J Virol* **84**, 6007–6017.

[17] Curtin JF, Liu N, Candolfi M, Xiong W, Assi H, Yagiz K, Edwards MR, Michelsen KS, Kroeger KM, Liu C, et al. (2009). HMGB1 mediates endogenous TLR2 activation and brain tumor regression. *PLoS Med* **6**, e10.

[18] Castro MG, Candolfi M, Kroeger K, King GD, Curtin JF, Yagiz K, Mineharu Y, Assi H, Wibowo M, Ghulam Muhammad AK, et al. (2011). Gene therapy and targeted toxins for glioma. *Curr Gene Ther* **11**, 155–180.

[19] Ali S, King GD, Curtin JF, Candolfi M, Xiong W, Liu C, Puntel M, Cheng Q, Prieto J, Ribas A, et al. (2005). Combined immunostimulation and conditional cytotoxic gene therapy provide long-term survival in a large glioma model. *Cancer Res* **65**, 7194–7204.

[20] Candolfi M, Curtin JF, Yagiz K, Assi H, Wibowo MK, Alzadeh GE, Foulad D, Muhammad AG, Salehi S, Keech N, et al. (2011). B cells are critical to T-cell–mediated antitumor immunity induced by a combined immune-stimulatory/conditionally cytotoxic therapy for glioblastoma. *Neoplasia* **13**, 947–960.

[21] Watowich SS and Liu YJ (2010). Mechanisms regulating dendritic cell specification and development. *Immunol Rev* **238**, 76–92.

[22] Curtin JF, King GD, Barcia C, Liu C, Hubert FX, Guillonneau C, Josien R, Anegon I, Lowenstein PR, and Castro MG (2006). *Fms*-like tyrosine kinase 3 ligand recruits plasmacytoid dendritic cells to the brain. *J Immunol* **176**, 3566–3577.

[23] Kim R, Emi M, Tanabe K, and Arihiro K (2007). Potential functional role of plasmacytoid dendritic cells in cancer immunity. *Immunology* **121**, 149–157.

[24] Hartmann E, Wollenberg B, Rothenfusser S, Wagner M, Wellisch D, Mack B, Giese T, Gires O, Endres S, and Hartmann G (2003). Identification and functional analysis of tumor-infiltrating plasmacytoid dendritic cells in head and neck cancer. *Cancer Res* **63**, 6478–6487.

[25] Wei S, Kryczek I, Zou L, Daniel B, Cheng P, Mottram P, Curiel T, Lange A, and Zou W (2005). Plasmacytoid dendritic cells induce $CD8^+$ regulatory T cells in human ovarian carcinoma. *Cancer Res* **65**, 5020–5026.

[26] Curiel TJ, Cheng P, Mottram P, Alvarez X, Moons L, Evdemon-Hogan M, Wei S, Zou L, Kryczek I, Hoyle G, et al. (2004). Dendritic cell subsets differentially regulate angiogenesis in human ovarian cancer. *Cancer Res* **64**, 5535–5538.

[27] Liu YJ (2005). IPC: professional type 1 interferon-producing cells and plasmacytoid dendritic cell precursors. *Annu Rev Immunol* **23**, 275–306.

[28] Southgate T, Kroeger KM, Liu C, Lowenstein PR, and Castro MG (2008). Gene transfer into neural cells *in vitro* using adenoviral vectors. *Curr Protoc Neurosci* **Chapter 4**, Unit 4.23.

[29] Ali S, Curtin JF, Zirger JM, Xiong W, King GD, Barcia C, Liu C, Puntel M, Goverdhana S, Lowenstein PR, et al. (2004). Inflammatory and anti-glioma effects of an adenovirus expressing human soluble *Fms*-like tyrosine kinase 3 ligand (hsFlt3L): treatment with hsFlt3L inhibits intracranial glioma progression. *Mol Ther* **10**, 1071–1084.

[30] Hatanaka K, Suzuki K, Miura Y, Yoshida K, Ohnami S, Kitade Y, Yoshida T, and Aoki K (2004). Interferon-α and antisense K-*ras* RNA combination gene therapy against pancreatic cancer. *J Gene Med* **6**, 1139–1148.

[31] Colamonici OR, Domanski P, Sweitzer SM, Larner A, and Buller RM (1995). Vaccinia virus *B18R* gene encodes a type I interferon-binding protein that blocks interferon α transmembrane signaling. *J Biol Chem* **270**, 15974–15978.

[32] Gerdes CA, Castro MG, and Lowenstein PR (2000). Strong promoters are the key to highly efficient, noninflammatory and noncytotoxic adenoviral-mediated transgene delivery into the brain *in vivo*. *Mol Ther* **2**, 330–338.

[33] Candolfi M, Curtin JF, Nichols WS, Muhammad AG, King GD, Pluhar GE, McNiel EA, Ohlfest JR, Freese AB, Moore PF, et al. (2007). Intracranial glioblastoma models in preclinical neuro-oncology: neuropathological characterization and tumor progression. *J Neurooncol* **85**, 133–148.

[34] Curtin JF, Candolfi M, Fakhouri TM, Liu C, Alden A, Edwards M, Lowenstein PR, and Castro MG (2008). Treg depletion inhibits efficacy of cancer immunotherapy: implications for clinical trials. *PLoS One* **3**, e1983.

[35] Ghulam Muhammad AK, Candolfi M, King GD, Yagiz K, Foulad D, Mineharu Y, Kroeger KM, Treuer KA, Nichols WS, Sanderson NS, et al. (2009). Antiglioma immunological memory in response to conditional cytotoxic/immune-stimulatory gene therapy: humoral and cellular immunity lead to tumor regression. *Clin Cancer Res* **15**, 6113–6127.

[36] Charles J, Chaperot L, Salameire D, Di Domizio J, Aspord C, Gressin R, Jacob MC, Richard MJ, Beani JC, Plumas J, et al. (2010). Plasmacytoid dendritic cells and dermatological disorders: focus on their role in autoimmunity and cancer. *Eur J Dermatol* **20**, 16–23.

[37] McKenna K, Beignon AS, and Bhardwaj N (2005). Plasmacytoid dendritic cells: linking innate and adaptive immunity. *J Virol* **79**, 17–27.

[38] Hussain SF, Yang D, Suki D, Aldape K, Grimm E, and Heimberger AB (2006). The role of human glioma-infiltrating microglia/macrophages in mediating antitumor immune responses. *Neuro Oncol* **8**, 261–279.

[39] Pinzon-Charry A, Ho CS, Laherty R, Maxwell T, Walker D, Gardiner RA, O'Connor L, Pyke C, Schmidt C, Furnival C, et al. (2005). A population of

HLA-DR$^+$ immature cells accumulates in the blood dendritic cell compartment of patients with different types of cancer. *Neoplasia* **7**, 1112–1122.

[40] King GD, Kroeger KM, Bresee CJ, Candolfi M, Liu C, Manalo CM, Muhammad AK, Pechnick RN, Lowenstein PR, and Castro MG (2008). Flt3L in combination with HSV1-TK–mediated gene therapy reverses brain tumor–induced behavioral deficits. *Mol Ther* **16**, 682–690.

[41] King GD, Muhammad AK, Curtin JF, Barcia C, Puntel M, Liu C, Honig SB, Candolfi M, Mondkar S, Lowenstein PR, et al. (2008). Flt3L and TK gene therapy eradicate multifocal glioma in a syngeneic glioblastoma model. *Neuro Oncol* **10**, 19–31.

[42] Mahnke K, Qian Y, Knop J, and Enk AH (2003). Induction of CD4$^+$/CD25$^+$ regulatory T cells by targeting of antigens to immature dendritic cells. *Blood* **101**, 4862–4869.

[43] Vermi W, Bonecchi R, Facchetti F, Bianchi D, Sozzani S, Festa S, Berenzi A, Cella M, and Colonna M (2003). Recruitment of immature plasmacytoid dendritic cells (plasmacytoid monocytes) and myeloid dendritic cells in primary cutaneous melanomas. *J Pathol* **200**, 255–268.

[44] Schettini J and Mukherjee P (2008). Physiological role of plasmacytoid dendritic cells and their potential use in cancer immunity. *Clin Dev Immunol* **2008**, 106321.

[45] King GD, Muhammad AK, Larocque D, Kelson KR, Xiong W, Liu C, Sanderson NS, Kroeger KM, Castro MG, and Lowenstein PR (2011). Combined Flt3L/TK gene therapy induces immunological surveillance which mediates an immune response against a surrogate brain tumor neoantigen. *Mol Ther* **19**, 1793–1801.

[46] Liu C, Lou Y, Lizee G, Qin H, Liu S, Rabinovich B, Kim GJ, Wang YH, Ye Y, Sikora AG, et al. (2008). Plasmacytoid dendritic cells induce NK cell–dependent, tumor antigen–specific T cell cross-priming and tumor regression in mice. *J Clin Invest* **118**, 1165–1175.

[47] Palumbo R, Sampaolesi M, De Marchis F, Tonlorenzi R, Colombetti S, Mondino A, Cossu G, and Bianchi ME (2004). Extracellular HMGB1, a signal of tissue damage, induces mesoangioblast migration and proliferation. *J Cell Biol* **164**, 441–449.

[48] Yu M, Wang H, Ding A, Golenbock DT, Latz E, Czura CJ, Fenton MJ, Tracey KJ, and Yang H (2006). HMGB1 signals through toll-like receptor (TLR) 4 and TLR2. *Shock* **26**, 174–179.

[49] Fuchsberger M, Hochrein H, and O'Keeffe M (2005). Activation of plasmacytoid dendritic cells. *Immunol Cell Biol* **83**, 571–577.

[50] Tsugawa T, Kuwashima N, Sato H, Fellows-Mayle WK, Dusak JE, Okada K, Papworth GD, Watkins SC, Gambotto A, Yoshida J, et al. (2004). Sequential delivery of interferon-α gene and DCs to intracranial gliomas promotes an effective antitumor response. *Gene Ther* **11**, 1551–1558.

[51] De Palma M, Mazzieri R, Politi LS, Pucci F, Zonari E, Sitia G, Mazzoleni S, Moi D, Venneri MA, Indraccolo S, et al. (2008). Tumor-targeted interferon-α delivery by Tie2-expressing monocytes inhibits tumor growth and metastasis. *Cancer Cell* **14**, 299–311.

[52] Palma G, De Laurenzi V, De Marco M, Barbieri A, Petrillo A, Turco MC, and Arra C (in press). Plasmacytoids dendritic cells are a therapeutic target in anticancer immunity. *Biochim Biophys Acta*.

[53] Aspord C, Charles J, Leccia MT, Laurin D, Richard MJ, Chaperot L, and Plumas J (2010). A novel cancer vaccine strategy based on HLA-A*0201 matched allogeneic plasmacytoid dendritic cells. *PLoS One* **5**, e10458.

[54] Vermi W, Soncini M, Melocchi L, Sozzani S, and Facchetti F (2011). Plasmacytoid dendritic cells and cancer. *J Leukoc Biol* **90**, 681–690.

[55] Lonsdorf AS, Kuekrek H, Stern BV, Boehm BO, Lehmann PV, and Tary-Lehmann M (2003). Intratumor CpG-oligodeoxynucleotide injection induces protective antitumor T cell immunity. *J Immunol* **171**, 3941–3946.

[56] Wolf IH, Kodama K, Cerroni L, and Kerl H (2007). Nature of inflammatory infiltrate in superficial cutaneous malignancies during topical imiquimod treatment. *Am J Dermatopathol* **29**, 237–241.

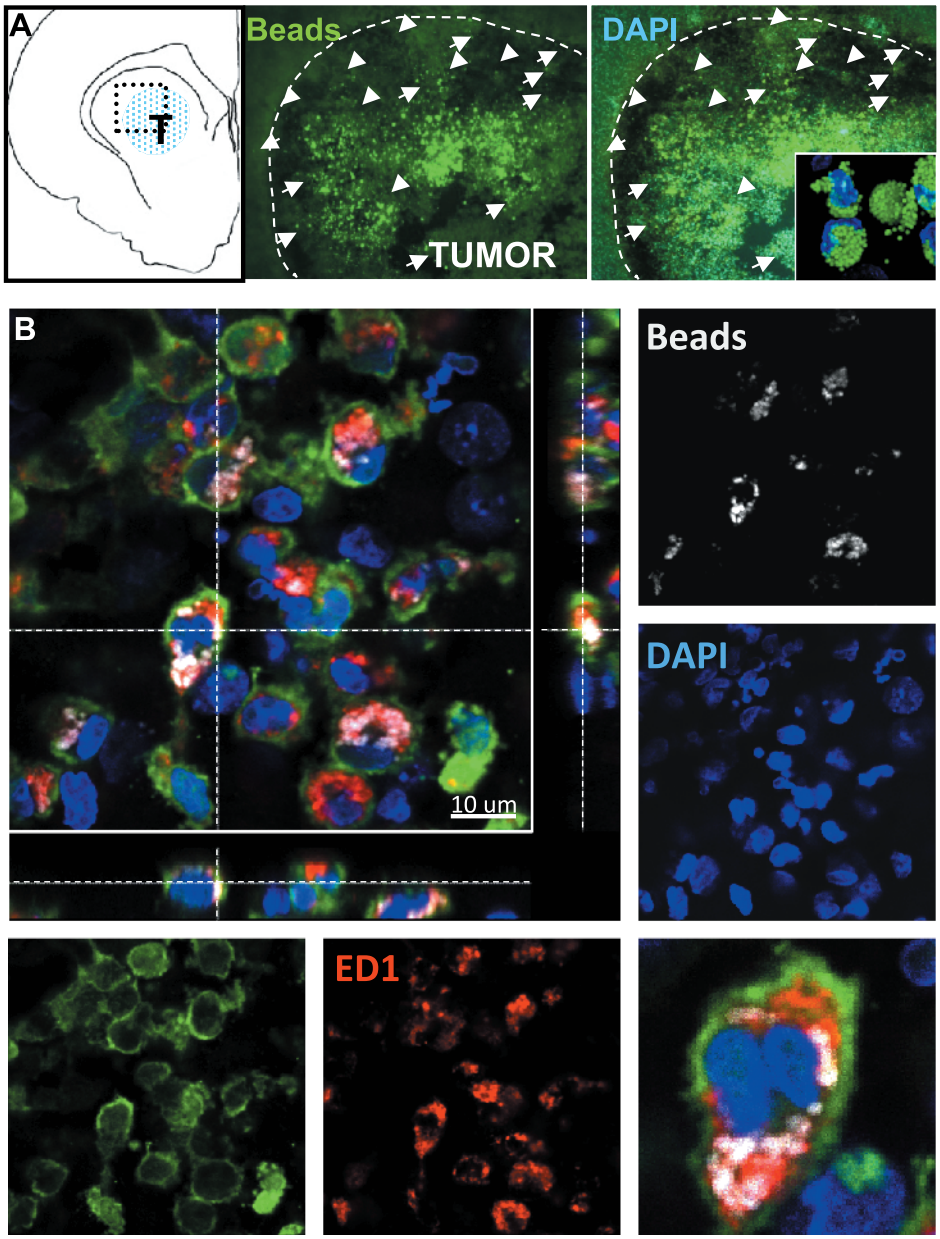

Figure W1. Bead internalization by ED1^{+} Iba1^{+} cells. Three days after treatment with Ad.TK + Ad.Flt3L, tumor-bearing rats were injected intratumorally with fluorescent microbeads. Two days later, the brains' immune cells were detected by immunofluorescence. (A) Arrows pointing cells containing beads within the brain tumor. Broken line indicates tumor border. Inset shows high-magnification microphotograph of cells containing beads within the tumor mass. (B) Confocal microphotograph showing tumor-infiltrating cells expressing the macrophage and microglia cell markers ED1 (red) and Iba1 (green) and containing beads (white) in the cytoplasm. Nuclei were stained with DAPI (blue).

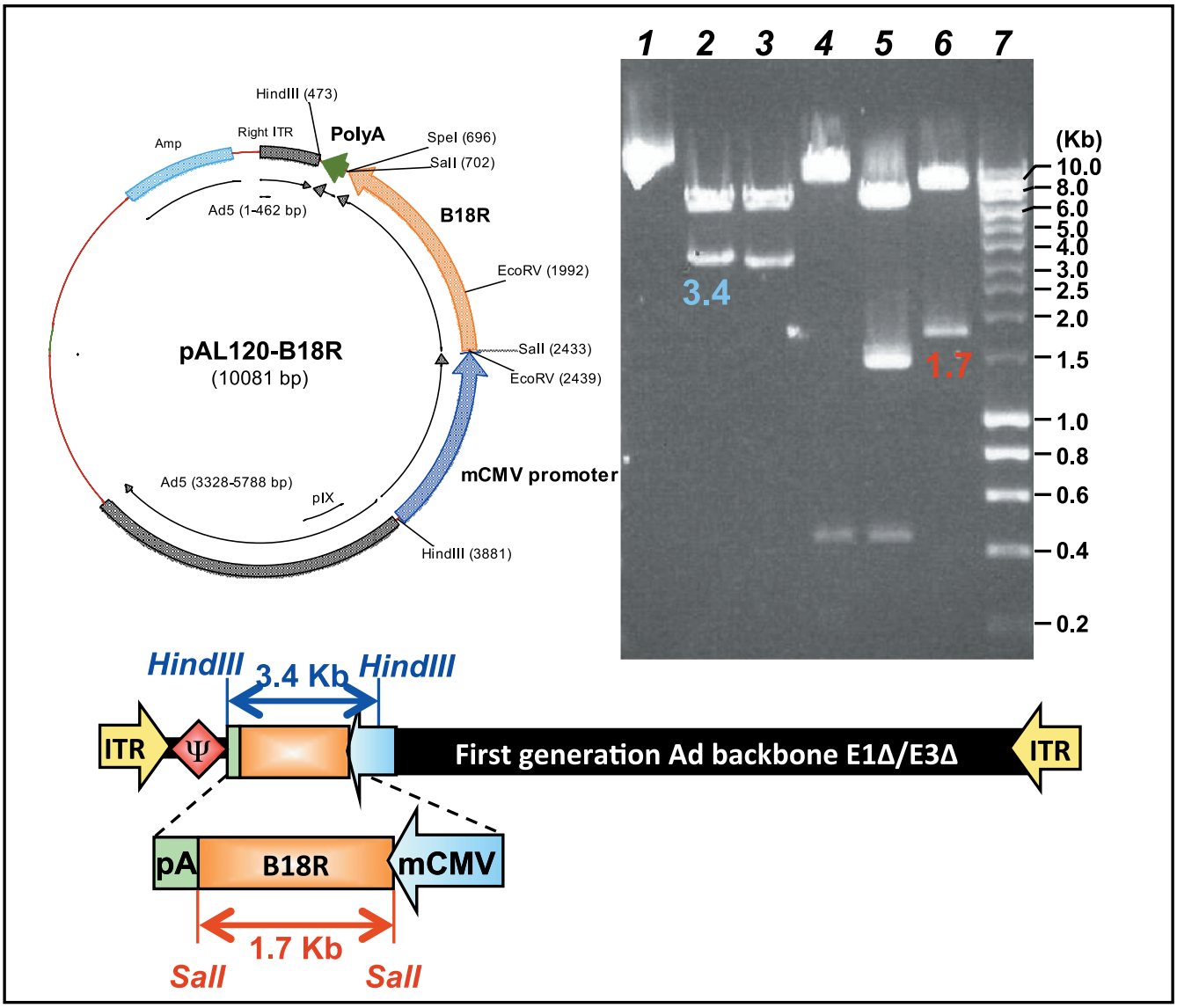

Figure W2. Construction of Ad.B18R. Adenoviral shuttle plasmid pAL120-B18R encoding the Vaccinia virus B18R cDNA (orange) that encodes a decoy receptor for IFN-α, which inhibits its function. Transgene expression is driven by the powerful murine cytomegalovirus promoter (mCMV, blue). Important restriction sites are indicated. Agarose gel electrophoresis and restriction map analysis of pAL120-B18R plasmid DNA to check for expected band sizes are shown. Lanes are as follows: lane 1, Hyladder 10 kb (Denville Scientific, Metuchen, NJ; corresponding sizes are labeled to the right of the gel); lane 2, uncut; lane 3, *Hin*dIII; lane 4, *Hin*dIII + *Spe*I; lane 5, *Eco*RV; lane 6, *Eco*RV + *Hin*dIII; lane 7, *Sal*I; lane 8, hyperladder 1. The colored fragments correspond to the indicated fragments in the schematic of Ad-mCMV-B18R vector genome linear depiction.

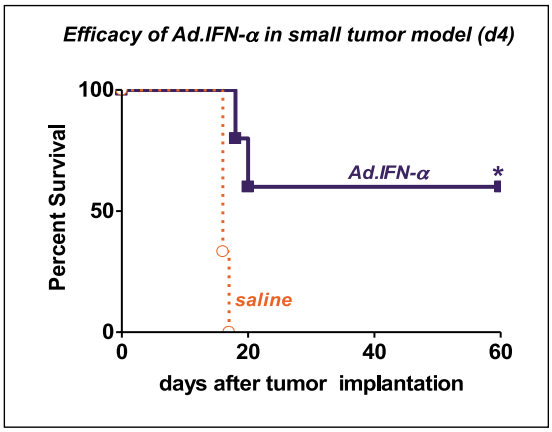

Figure W3. Efficacy of intratumoral injection of Ad.TK in combination with Ad.IFN-α. Tumor-bearing rats were treated 4 days after tumor implantation by intratumoral injection of saline or Ad.IFN-α or saline. *$P < .05$ *versus* saline. Mantel log-rank test.

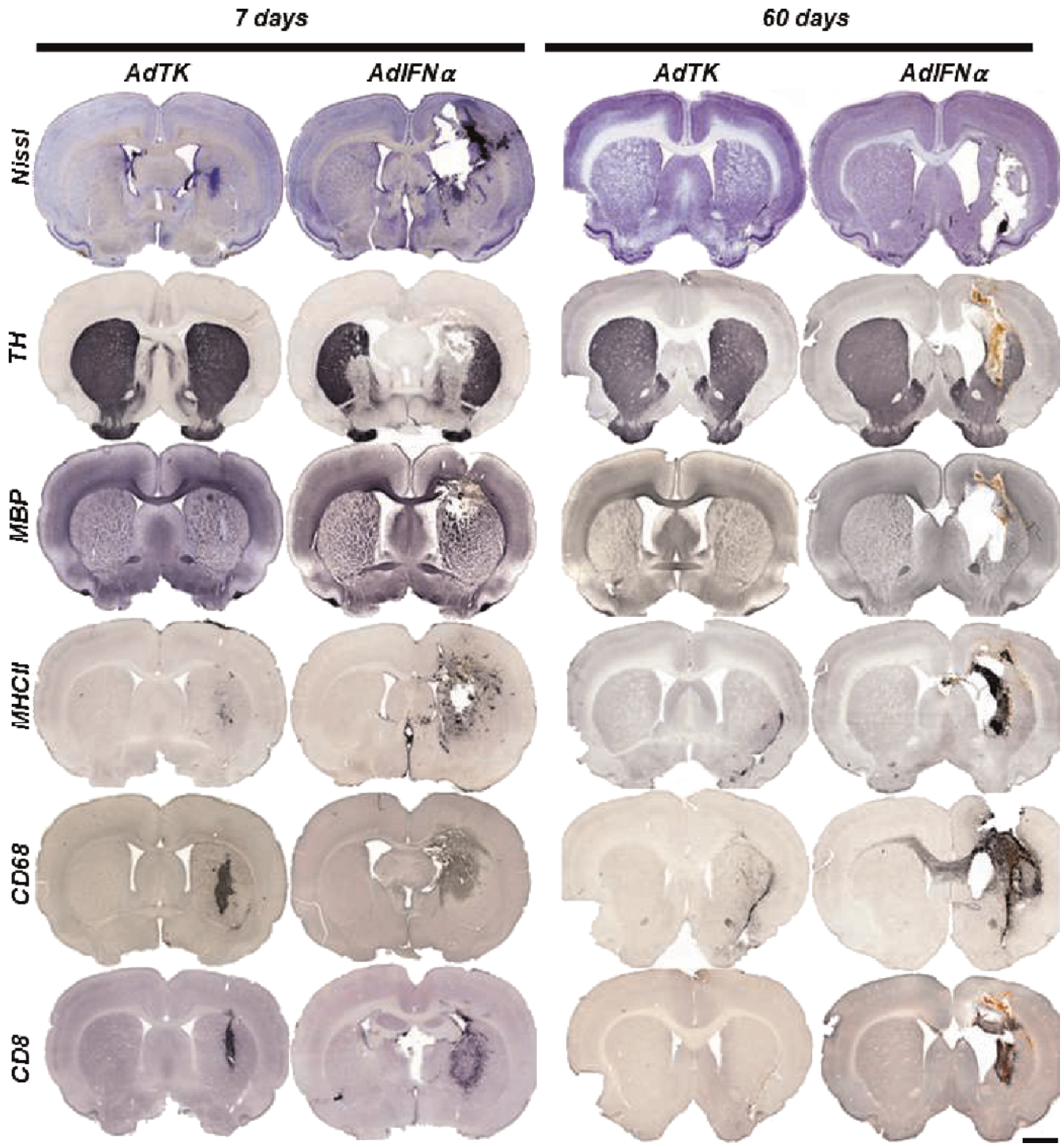

Figure W4. Acute neurotoxicity after Ad.IFN-α injection in naive rat brain. Naive Lewis rats were injected in the striatum with Ad.IFN-α or Ad.TK. Rats treated with Ad.TK received GCV treatment daily. Seven and 60 days after vector delivery, neuropathologic analysis of the brain was assessed by Nissl staining and immunocytochemistry using antibodies against TH, MBP, MHC II, CD68 (macrophages/activated microglia), and CD8α (T cells). Scale bar, 2 mm.

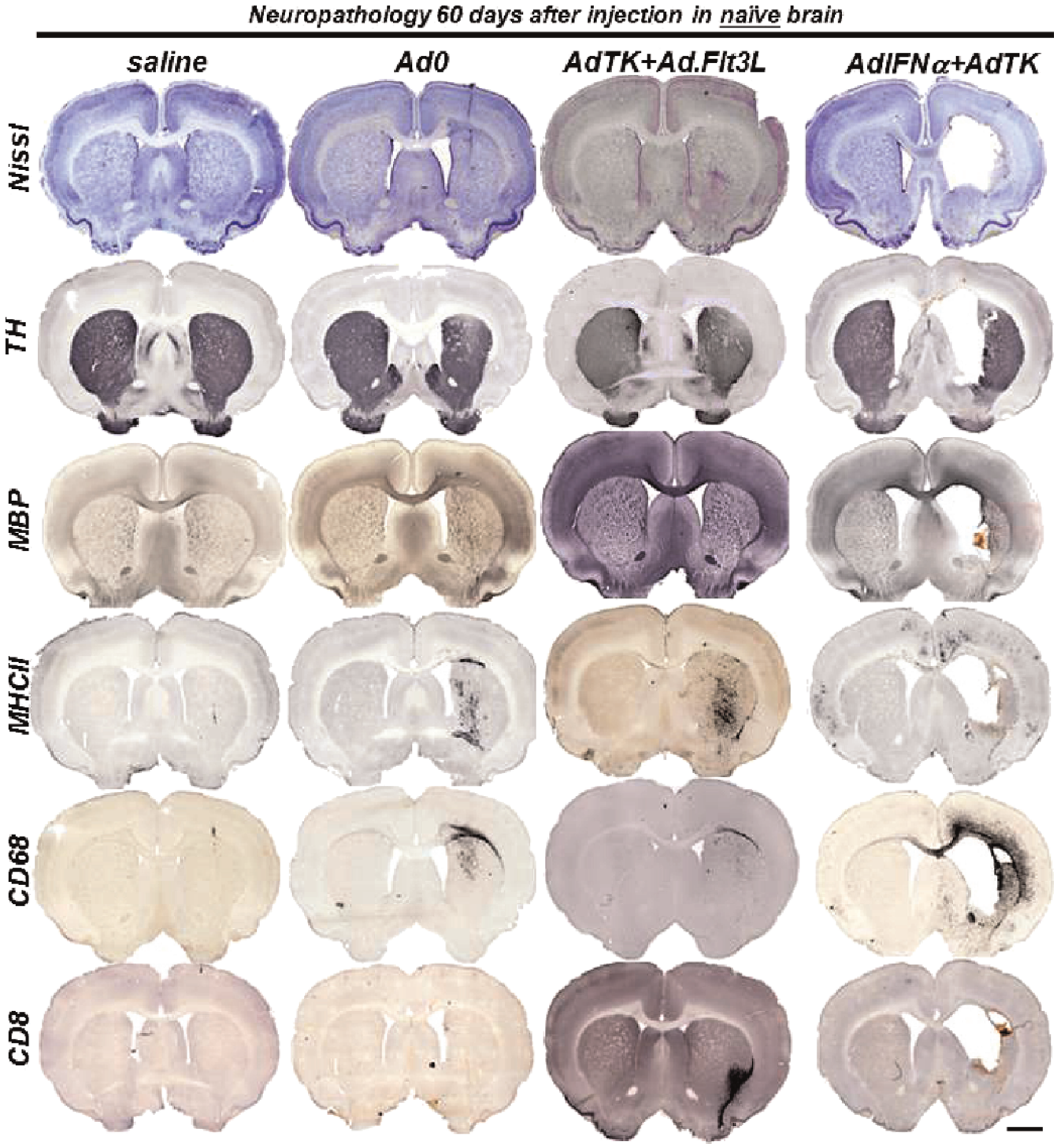

Figure W5. Chronic neuropathologic changes after Ad.IFN-α injection in naive rat brain. Naive Lewis rats were injected in the striatum with Ad.IFN-α or Ad.Flt3L and Ad-TK. As controls, rats received saline or Ad.0. Rats treated with Ad-TK received GCV treatment daily. Sixty days after vector delivery, neuropathologic analysis of the brain was assessed by Nissl staining and immunocytochemistry using antibodies against TH, MBP, MHC II, CD68 (macrophages/activated microglia) and CD8α (T cells). Scale bar, 2 mm.